A New Model-Based Approach for the Development of Freeze-Drying Cycles Using a Small-Scale Freeze-Dryer

Journal of Pharmaceutical Sciences
https://jpharmsci.org/article/S0022-3549(23)00194-6/fulltext
https://doi.org/10.1016/j.xphs.2023.05.007

A new model-based approach for the development of freeze-drying cycles using a small-scale freeze-dryer

Ambra Massei, Davide Fissore

Dipartimento di Scienza Applicata e Tecnologia,
Politecnico di Torino,
corso Duca degli Abruzzi 24, 10129 Torino

Abstract

This paper presents a model-based approach for the design of the primary drying stage of a freeze-drying process using a small-scale freeze-dryer (MicroFD® by Millrock Technology Inc.). Gravimetric tests, coupled with a model of the heat transfer to the product in the vials that account also for the heat exchange between the edge vials and the central vials, are used to infer the heat transfer coefficient from the shelf to the product in the vial (K_v), that is expected to be (almost) the same in different freeze-dryers. Differently from other approaches previously proposed, the operating conditions in MicroFD® are not chosen to mimic the dynamics of another freeze-dryer: this allows saving time and resources as no experiments are needed in the large-scale unit, and no additional tests in the small-scale unit, apart from the three gravimetric tests usually needed to assess the effect of chamber pressure on K_v. With respect to the other model parameter, R_p, the resistance of the dried cake to mass transfer, it is not influenced by the equipment and, thus values obtained in a freeze-dryer may be used to simulate the drying in a different unit, provided the same filling conditions are used, as well as the same operating conditions in the freezing stage, and cake collapse (or shrinkage) is avoided. The method was validated considering ice sublimation in two types of vials (2R and 6R) and at different operating conditions (6.7, 13.3 and 26.7 Pa), with the freeze-drying of a 5% w/w sucrose solution as a test case. An accurate estimate for both K_v and R_p was obtained with respect to the values obtained in a pilot-scale equipment, determined through independent tests for validation purposes. Simulation of the product temperature and drying time in a different unit was then possible, and results were validated experimentally.

Keywords

Freeze-drying, Micro freeze-dryer, Mathematical modelling, Scale-up, Optimization

List of abbreviations

API	Active Pharmaceutical Ingredient
FDA	Food and Drug Administration

Nomenclature

A	Mass transfer experimental parameter to determine R_p, s^{-1}
A_L	Exchange area between the LyoSim® and the external layer, m^2
$A_{v,b}$	Cross-section area of the vial, m^2
$A_{v,i}$	Cross-section area of the product in the vial, m^2
A_{12}	Heat exchange area vial-to-vial, m^2
a_0	Mass transfer experimental parameter to determine r_e/τ, m
a_1	Mass transfer experimental parameter to determine r_e/τ, -
B	Mass transfer experimental parameter to determine R_p, m^{-1}
C	Heat transfer experimental parameter to determine K_v, W m^{-2} K^{-1}
c_p	Specific heat of ice, J $kg^{-1}K^{-1}$
c_w	Water vapor concentration, mol m^{-3}
D	Heat transfer experimental parameter to determine K_v, W $m^{-1}K^{-1}Pa^{-1}$
D_e	Effective Knudsen diffusivity, m^2 s^{-1}
E	Heat transfer experimental parameter to determine K_v, Pa^{-1}
ΔH_S	Enthalpy of ice sublimation, J kg^{-1}
I_{xy}	Convention used to identify the integral, K s
J_q	Heat flux to the product, W m^{-2}
J_w	Mass flux, kg s^{-1} m^{-2}
K	Constant for the calculation of the Knudsen diffusivity, m $s^{-1}K^{-0.5}$
KK	Constant for the calculation of the mass transfer resistance R_p, kg $Pa^{-1}s^{-1}$

64	K_L	Heat transfer coefficient between the LyoSim® and the external layer, W $m^{-2}K^{-1}$
65	K_v	Heat transfer coefficient between the shelf and the product in the vial, W $m^{-2}K^{-1}$
66	K_v^*	Effective heat transfer coefficient between the shelf and the product in the vial,
67	W $m^{-2}K^{-1}$	
68	K_{12}	Heat transfer coefficient between two nearby vials, W $m^{-2}K^{-1}$
69	K_{12}^*	Effective heat transfer coefficient between two nearby vials, W $m^{-2}K^{-1}$
70	L	Thickness of the product, m
71	M_w	Water molecular weight, kg mol^{-1}
72	Δm	Weight loss in the vial during the gravimetric test, kg
73	m	Mass of sublimated water at a generic instant, kg
74	m_{sub}	Total mass of sublimated water during the process, kg
75	m_w^*	Instantaneous amount of sublimated ice mass, kg
76	Δm	Weight loss in the external vials during the gravimetric test, kg
77	N_{lat}	Number of vials directly in contact with the external layer, -
78	ΔP	Water vapor pressure difference, Pa
79	P_c	Total chamber pressure, Pa
80	p_w	Water vapor partial pressure, Pa
81	Q	Total amount of heat received by the product from the shelf, J
82	Q_{ACC}	Amount of heat accumulated by the product during the process, J
83	Q_{base}	Amount of heat received by the vials from the shelf, J
84	Q_{LAT}	Amount of heat exchanged by a central vial with the surrounding ones, J
85	Q_{LyoSim}	Amount of heat received by the external layer from the LyoSim®, J
86	Q_{subl}	Amount of heat lost by the vials due to sublimation, J
87	R	Ideal gas constant, J $mol^{-1}K^{-1}$

88	R_p	Resistance of the dried cake to the vapor, Pa s m^2 kg^{-1}
89	$R_{p,0}$	Mass transfer experimental parameter to determine R_p, m s^{-1}
90	r_e	Effective pore radius, m
91	T	Product temperature profile, K
92	t	Time, s
93	Δt	Duration of the ice sublimation stage, s
94	T_B	Temperature of the product at the bottom of the vial, K
95	T_L	Temperature of the silicone-based heat transfer fluid is pumped through the ring, K
96	T_S	Temperature of the silicone-based heat transfer fluid is pumped through the shelf, K
97		
98	Greeks	
99	ε	Void fraction, -
100	λ	Thermal conductivity, W $m^{-1}K^{-1}$
101	ρ	Density, kg m^{-3}
102	τ	Tortuosity of the solid matrix, -
103		
104	Subscripts	
105	*c*	Drying chamber
106	*dried*	Dried product
107	*frozen*	Frozen product
108	*I*	Interface of sublimation
109	*ice*	Ice
110	1, ext	External layer of vials
111	2, int	Internal layer of vials
112	$\bar{}$	Mean value

113 . Heat flux

1. Introduction

Freeze-drying is a process widely used to provide physical and chemical stability to biopharmaceuticals during shipping and long-term storage through three different steps. Firstly, the containers, usually vials, with the formulation containing the active pharmaceutical ingredient (API), are loaded into the freeze-dryer. The solution is frozen and, then, water is removed by sublimation (primary drying) by lowering the pressure and by increasing the temperature of the shelf, as ice sublimation is endothermic. Lastly, the bounded water is removed (secondary drying) by increasing again the temperature of the shelf to accelerate water desorption. So, at the end of the freeze-drying process the active ingredient is locked into a porous solid matrix, which allows for slowing down chemical-physical degradation reactions.[1,2]

The main advantage of freeze-drying over other drying techniques is the ability to treat thermolabile products since it operates at low pressures and temperatures. However, the freeze-drying is a long and expensive process. The primary drying is the longest and most critical phase. The aqueous formulations often contain amorphous or crystalline excipients. Thus, during this step it is necessary to assure that the product temperature remains below a certain critical value, namely, respectively, the glass transition temperature or the eutectic temperature, to prevent the collapse of the cake or the product melting. A careful identification of the design space is required.[3,4] The FDA defined it as "*the multidimensional combination of input variables and process parameters that have been demonstrated to provide assurance of quality*".[5] Here, the input variables are the operating conditions of the freeze-drying process: the temperature of the heating fluid and the pressure in the drying chamber. The adequate combination of these two parameters is often obtained through an extended experimental campaign with the goal to meet the process needs (i.e. the target residual moisture and the temperature of the product during processing) and, if possible, to minimize drying time. Mathematical modeling was proven to be effective to get the design space[6-8], but, in all cases, the model parameters, K_v and R_p, used to model, respectively, the heat transfer to the product in the vial and the mass transfer from the product to the chamber, must be estimated experimentally. This is time

consuming, due to the length of the cycle, and also the loading/unloading and sample preparation operations play an important role. Moreover, one challenge for researchers is represented by the limited availability of the active pharmaceutical ingredient, which is a relevant cost for pharmaceutical industry.[9,10]

To address these issues, a different approach using a small-scale freeze-dryer could be helpful. In fact, the time required for batch preparation is reduced and the amount of API is minimized in this case, thus leading to a more rapid drug development stage and, finally, to a faster introduction of drugs into the market. In this framework it would be really useful to get similar dynamics in the different situations: laboratory, pilot and manufacturing scale. The major difficulty for the scale-down/scale-up procedures is given by the intrinsic heterogeneity of the freeze-drying process.[11-13] As highlighted in previous studies, the heat transfer in a batch does not occur uniformly: the edge vials, unlike the central ones, are heated by radiation from chamber walls and by conduction in the gas surrounding the vials.[14,15] As a consequence, the drying time is shorter (and the product temperature is higher) in the edge vials with respect to the central ones. Also vial packing density may influence heat transfer to the vials of the batch: this is due to a different number of vials surrounding the monitored one, that affects the heat transfer to the lateral surface of vials during primary drying as each vial acts as a "heat sink", due to ice sublimation that is an endothermic phenomenon, resulting in a cooling effect.[16] This issue was investigated also by Elhers et al.[17], who focused also on the inter-vials distance, pointing out that, in the considered layout, energy transfer by gas conduction enables the cooling effect of a neighboring vial over a distance up to 10 mm. While in an industrial freeze-dryer the fraction of edge vials is limited, on a small-scale its impact is significantly greater.[18,15]

Obeidat et *al*. developed a prototype version of a mini-freeze dryer with adjustable chamber wall temperatures able to emulate the behavior in a much larger freeze-dryer by using only 7 vials.[19] Also, another prototype was investigated by introducing in the drying chamber a cylindrical temperature-controlled wall. The main limitation of both configurations was the edge vial effect and a non-consistent batch uniformity with respect to temperature. A different system was proposed by

Thompson et *al*.: the MicroFD® (Millrock Technology Inc., Kingston, NY).[20] In this equipment the external vials of the small batch are surrounded by an aluminum ring (LyoSim®) whose temperature may be adjusted independently from that of the shelf. The ring has the role to mimic the presence of an additional row of vials: by changing its temperature, the edge effect in the batch may be minimized.[20]

Goldman et *al*. investigated this device by loading a batch of 7 vials (20R).[21] They demonstrated the ability of the MicroFD®, through a proper selection of the temperature of the ring, to get a batch where the dynamics of central or edge vials of a different unit may be reproduced. Other studies of Fissore et. *al.* evidenced that, by means of a proper tuning of the ring temperature, the dynamics of central vials of a larger unit may be reproduced and, thus, by means of tests carried out in MicroFD® it was possible to accurately estimate the model parameters K_v and R_p, that could be then used to simulate *in silico* product evolution in a pilot-scale unit (REVO® by Millrock Technology Inc., Kingson, NY).[9,22] They analyzed 10% w/w sucrose and 5% w/w mannitol aqueous solutions in different vials (6R and 20R), focusing the study on product temperature and batch drying time. They assessed that for ring temperature offset values ranging from -1°C to -5°C the product temperature was very close to the one obtained in the central vials processed in the REVO® freeze-dryer.

It has to be highlighted that in all these studies it was needed to carry out one or more gravimetric tests in the large-scale unit, to get knowledge about the heat transfer from the chamber to the vial (K_v) that, than, has to be replicated in MicroFD® by a proper adjustment of the ring temperature, thus making necessary other gravimetric tests in this unit. Once the equivalence of heat transfer has been obtained, then product (API) drying may be investigated experimentally in MicroFD®, i.e. the effect of the temperature of the heat transfer fluid pumped through the shelf, commonly referred to as shelf temperature, and chamber pressure on drying time and product temperature. This method allows using a small amount of API for cycle development and optimization without the necessity of using a larger scale freeze-dryer (partially loaded), as few vials are loaded into MicroFD®, but time is needed to get K_v in the large-scale unit, and to find the ring temperature that provides equivalent heat exchange in

the MicroFD®, although batch preparation time in MicroFD® is very short.

This paper shows an innovative method to use the data obtained in MicroFD® to design a freeze-drying cycle for a larger scale unit, without any need for additional tests in this second freeze-dryer, and without any optimization of the ring temperature. Tests in a larger-scale unit (REVO®) were carried out for validation purposes, but in the proposed pipeline they are not necessary. Unlike before, gravimetric tests were carried out by always setting the temperature of the heat transfer fluid pumped through the ring equal to that of the fluid pumped through the shelf: by this way, we are not sure to be able to get a uniform batch, and to replicate the behavior of any group of vials of a different unit. Therefore, the model used to process the data encompasses a vial-to-vial heat exchange, thus allowing to discriminate between the heat exchange from the shelf to the vial, which is expected not to be influenced by the freeze-dryer, and the heat contribution from the edge vials. Modeling framework is shown in Section 2 of this paper, while results obtained processing a 5% sucrose solution in different type of vials (2R and 6R) are presented and discussed in the following Section, aiming to point out strengths and drawbacks of this approach.

It has to be remarked that the proposed method is focused on the central vials of the batch, that constitute the majority of the batch and are characterized by the longest drying time. The temperature in the edge vials is higher than in the central ones, and this is usually managed by selecting a proper safety margin, i.e. lowering the selected temperature of the fluid pumped through the shelf of a couples of degrees, or setting a target temperature for the central vials a couple of degrees lower than the effective limit value. In some cases, the edge vials may be empty, in such a way that no safety margin is needed. In all cases, drying time in edge vials is shorter than in central vials and, thus, this does not represent an issue when optimizing a cycle.

2. Materials and Methods

2.1 Freeze-drying units

A laboratory-scale freeze-dryer, namely MicroFD®, and a pilot-scale freeze-dryer, namely REVO®,

by Millrock Technology Inc. (Kingston, NY) were used to carry out the experimental tests.

The MicroFD® device is characterized by a circular shelf of 6 in diameter. A silicone-based heat transfer fluid is pumped through the shelf to heat or cool the product (depending on the phase) by operating at temperatures ranging from -60°C to +60°C. There is an independent thermal circuit, LyoSim®, used to control the temperature of the aluminum ring. The temperature of LyoSim® can be adjusted by setting an offset from the product temperature, measured through thermocouples placed in some of the vials of the batch, or from the temperature of the fluid pumped through the shelf (T_S). Negative offset values compensate for the additional heat due to the edge effect and allow the dynamics of central vials of a larger unit to be simulated. The dimensions of LyoSim® can be appropriately adjusted, depending on the type of vials used, in order to guarantee the contact (and, thus, an efficient heat exchange) between the ring and the external vials of the batch. As an example, it is possible to load 37 each 2R vials or 19 each 6R vials.

The REVO® device is a pilot-scale freeze-dryer characterized by up to 12 sq ft of shelf area. Experiments with 6R vials involved 163 vials arranged according to a hexagonal array: 13 rows containing either 13 or 12 vials. Instead, for the 2R vials, 245 vials were used: 14 rows containing either 18 or 17 vials. Figure 1 shows the schematic arrangements of vials for the four kinds of tests conducted in this study. According to the target of this study, in the REVO® device only central vials are considered for cycle development.

Several T-type thermocouples (Tersid, Milano, Italy) were used during the tests in both units, paying attention to put them in close contact with the vial bottom. In particular, five thermocouples were used in the MicroFD® device: two monitored the temperature of the edge vials and the other three that of the central vials. Instead, three thermocouples were used for the REVO® freeze-dryer, monitoring the behavior of the central vials. Temperature probes positioning is also shown in Figure 1. In both devices the chamber pressure was monitored using a capacitive (Baratron 626A, MKS Instruments, Andover, USA) and a thermal conductivity (Pirani PSG-101-S, Bad Ragaz, Switzerland) pressure gauge.

244

245 *2.2 Product, vials and operating conditions*

246 For the study of the heat transfer process, gravimetric tests were carried out using only water, since
247 the heat transfer coefficient to the vials does not depend on the product. For the 6R vials the filling
248 volume was equal to 3 mL, while for the 2R vials it was equal to 1.5 mL. All the vials were weighted
249 using a XS-BL-224 balance (Nuova Tecnogalenica s.r.l., Cernusco sul Naviglio, Italy) and then
250 partially stoppered using an igloo stopper (NovaPure Chlorobutyl Igloo Stoppers, West Pharma,
251 Exton, PA). The offset of LyoSim® was set equal to 0°C with respect to T_S in these gravimetric test,
252 so the temperature of LyoSim® was always equal to T_S. During the freezing stage, T_S was set equal to
253 -50°C. After making sure that the product temperatures, measured by the different thermocouples,
254 had stabilized at around -50°C, the ice sublimation stage was activated by considering a holding time
255 of 180 minutes and setting the T_S at -10°C. In all tests, the shelf cooling rate was set at -1°C/min and
256 the heating rate at +1°C/min, in both freezing and sublimation stages. At the end of the described
257 cycle, atmospheric pressure in the chamber was restored and all the vials were manually closed. Then,
258 each vial was weighted again to calculate the weight loss, so the amount of ice sublimated during the
259 process. Three different pressures were tested: 6.7, 13.3 and 26.7 Pa.

260 Complete freeze-drying cycles were carried out using 5% w/w aqueous sucrose solution, both in 2R
261 and 6R vials, to estimate the resistance of the dried cake to vapor flow. Sucrose was purchased from
262 Fisher Chemical (Geel, Belgium). The solution was prepared using distilled water (demineralizer RO
263 30 CUBIC – Gamma 3 s.n.c., Castelverde, Italy). To ensure complete dissolution of the sugar in
264 water, the solution was stirred for 15 minutes using a magnetic stirrer. Then, the solution was filtered
265 using 0.45 μm hydrophilic filters (Labbox Labware S.L., Barcelona, Spain) and poured in either 6R
266 (3 mL per vial) or 2R (1.5 mL per vial) vials. These experiments were carried out both in the
267 MicroFD®, considering an offset for LyoSim temperature equal to -3°C, aiming to test the
268 performance of the method also in another case, and REVO® freeze-dryers. Also in this case, all vials
269 were partially stoppered using an igloo stopper (NovaPure Chlorobutyl Igloo Stoppers, West Pharma,

Exton, PA). The aim of these kind of tests was the acquisition of the product temperature profiles and of the ratio between the Pirani and Baratron pressure gauges signals to assess the end of primary drying.[23] In this case, the product temperature was monitored in four vials. The test was done only for the chamber pressure equal to 13.3 Pa and T_S was set to -10°C during the primary stage. The cooling phase was carried out by setting a ramp down to -50°C. In all tests, the shelf cooling rate was set at -1°C/min, and the heating rate at +1°C/min. Differently from the gravimetric tests, the holding phase of primary drying was not decided a priori, but the end of the cycle was suggested by the profile of the ratio between the Pirani and Baratron pressure gauges signals as a function of time. In other words, the atmospheric pressure in the chamber was restored when this ratio was about equal to 1, index of complete sublimation.

2.3 Mathematical Modelling

2.3.1 K_v calculation from gravimetric test carried out in a pilot-scale freeze-dryer

As underlined in Section 1, the primary drying phase is the longest and the most expensive step of the whole freeze-drying process. Since the radial thermal and composition gradients in each vial are usually negligible, a mono-dimensional model may be accurate enough to calculate the evolution of the product temperature and the time required to complete ice the sublimation.[24-28]

In each vial, the product receives heat from the fluid flowing into the shelf. The heat flux, J_q, is directly proportional to the difference between the temperature of the fluid flowing into the shelf, T_S, and the one of the product at the bottom of the vial, T_B, as shown in Eq. (1):

$$J_q = K_v \left(T_S - T_B \right) \quad (1)$$

The coefficient of proportionality, K_v, is the heat transfer coefficient between the product and the heating fluid inside the shelf, i.e. the shelf. Equation (1) is correct for the so called “central vials”, i.e. those vials located in the central part of the shelf, as they receive heat only from the shelf itself. Vials located at the edges of the shelf receive also an additional amount of heat, mainly due to radiation

from chamber walls: in this case eq. (1) is still used, but K_v has now to be regarded as an "effective" heat transfer coefficient, that allows obtaining the total heat flux to the vials considering the driving force (T_S-T_B).

The heat transferred to the product in the vials is used mainly for ice sublimation: heat accumulation in the vials is usually neglected due to the large thermal inertia of the product in the vial, that makes very slow the rise of temperature (i.e. the heat accumulation) in comparison with ice sublimation. Taking into account this assumption, in each gravimetric test used to get the value of K_v the total amount of heat received by the product can be calculated by Eq. (2):

$$Q = \Delta m \cdot \Delta H_S \tag{2}$$

as the weight loss in each vial (Δm) due to ice sublimation is measured, and the enthalpy of sublimation (ΔH_S) is known. The total amount of heat transferred to the vial can be also expressed by Eq. (3):

$$Q = K_v A_{v,b} \int_0^{\Delta t} (T_S - T_B) dt \tag{3}$$

where Δt is the duration of the ice sublimation step in the gravimetric run. By comparing Eq. (2) and Eq. (3), it is possible to get the parameter K_v:

$$K_v = \frac{\Delta m \cdot \Delta H_S}{A_{v,b} \int_0^{\Delta t} (T_S - T_B) dt} \tag{4}$$

Equation (4) may be used to calculate K_v from the data of weight loss (Δm) and product temperature (T_B) obtained in gravimetric test, e.g. in the REVO® freeze-dryer. When the weight loss (and product temperature) in central vials is considered, the true value of K_v is obtained. When the weight loss (and product temperature) in edge vials is considered, an effective value of K_v is obtained as the model assumes that all the heat is provided to the vials from the shelf, while for edge vials a certain fraction of heat arrives also from radiation and conduction in the external gas surrounding the vials.

2.3.2 K_v calculation from gravimetric test carried out in MicroFD® freeze-dryer

When performing the gravimetric test in MicroFD® a deeper analysis of the heat fluxes is required. As it is shown in Figure 2, the system may be simplified by considering two layers:

- The external layer, directly in contact with the ring, considered homogeneous (the first row in Figure 1 in dark grey).
- The internal layer, considered homogeneous.

Experimental measurements of temperature and weight loss allowed to validate this hypothesis. Figure 2 points out all the heat fluxes present in the MicroFD® freeze-dryer: the heat fluxes exchanged between each vial in the layer and the shelf, namely $\dot{Q}_{base,int}$ (for the internal layer) and $\dot{Q}_{base,ext}$ (for the external layer); the one between the LyoSim® and the external layer ($\dot{Q}_{LyoSim}$); the vial-to-vial term ($\dot{Q}_{LAT}$) and the sublimation terms, namely $\dot{Q}_{subl,int}$ (for the internal layer) and $\dot{Q}_{subl,ext}$ (for the external layer). If we carry out the gravimetric test in the MicroFD® freeze-dryer, the weight loss in each vial is measured, as well as the temperature in some vials (of the internal and of the external layer), and these fluxes may be calculated as outlined in the followings. In fact, $\dot{Q}_{base,int}$ and $\dot{Q}_{base,ext}$ may be calculated as shown in the following equations. At first, the total amount of heat received from the bottom may be expressed as:

$$Q_{base,int} = N_{int} K_v A_{v,b} \int_0^{\Delta t} \left(T_S - \bar{T}_2\right) dt = N_{int} K_v^* \int_0^{\Delta t} \left(T_S - \bar{T}_2\right) dt \quad (5)$$

$$Q_{base,ext} = N_{ext} K_v A_{v,b} \int_0^{\Delta t} \left(T_S - \bar{T}_1\right) dt = N_{ext} K_v^* \int_0^{\Delta t} \left(T_S - \bar{T}_1\right) dt \quad (6)$$

The integral is known as T_s is measured and $\bar{T}_1$ and $\bar{T}_2$ are the mean product temperature profiles, respectively in the external layer and in the internal one, all monitored during the test. They were considered equal to the average of temperatures measured by thermocouples in the outer and central vials. The two parameters, N_{int} and N_{ext}, refer, respectively to the number of vials in the internal layer and in the external one. They were added in the formulas to take into account that all the central or

external vials exchange heat with the shelf. The two values of the multiplicative factors change depending on the arrangement used. Specifically, the first layer is made up of 7 vials in the case of 6R vial and of 19 vials in case of 2R vials. Instead, the outer layer is made up of 12 vials in the case of 6R vials and of 18 vials for the 2R vials. Finally, the mean heat fluxes exchanged, $\dot{Q}_{base,int}$ and $\dot{Q}_{base,ext}$ are calculated by dividing the two amounts of heat by the duration of the ice sublimation step, here reported as Δt:

$$\dot{Q}_{base,int} = \frac{Q_{base,int}}{\Delta t},\ \dot{Q}_{base,ext} = \frac{Q_{base,ext}}{\Delta t} \tag{7}$$

With respect to the sublimation terms, i.e. $\dot{Q}_{subl,int}$ and $\dot{Q}_{subl,ext}$, the heat of sublimation can be expressed as the product between the enthalpy of sublimation, ΔH_S, and the amount of sublimated ice, $\overline{\Delta m_2}$, for the internal layer, and $\overline{\Delta m_1}$ for the external one. They represent, respectively, the average mass variations of the central and of the external vials. Therefore, the amounts of heat lost due to sublimation, $Q_{subl,int}$ and $Q_{subl,ext}$, and the corresponding heat fluxes ($\dot{Q}_{subl,int}$ and $\dot{Q}_{subl,ext}$) in the two groups of vials can be found by the following equations:

$$Q_{subl,int} = N_{int}\Delta H_s \overline{\Delta m_2},\ \dot{Q}_{subl,int} = \frac{Q_{subl,int}}{\Delta t} \tag{8}$$

$$Q_{subl,ext} = N_{ext}\Delta H_s \overline{\Delta m_1},\ \dot{Q}_{subl,ext} = \frac{Q_{subl,ext}}{\Delta t} \tag{9}$$

With respect to the vial-to-vial term, $\dot{Q}_{LAT}$, it is convenient to look at the Figure 3, where the zoom of the arrangement for the 6R vials in the MicroFD® is reported (All the following findings are valid also for the 2R arrangement by only changing the multiplicative factors in the formulas, as explained above). Each vial can be subdivided into six slices to better point out the vial-to-vial heat exchange. Focusing on the vials of the central layer it is possible to assess that:

1. The slices 3 and 4 of the vials in the central layer exchange heat with vials at the same temperature. Therefore, the net heat flux in these slices is zero. The heat flux for each slice is designed,

respectively, as $\dot{Q}_3$ and $\dot{Q}_4$.

2. The slices 1 and 6 of the vials in the central layer exchange heat with two vials of the external layer. The heat flux for each slice is designed, respectively, as $\dot{Q}_1$ and $\dot{Q}_6$. The two contributions are equal, so the total heat flux, for the two slices, is given by $2\dot{Q}_1$.
3. The slices 2 and 5 of the vials in the central layer exchange heat in a similar way, with a vial of the central layer, at the same temperature, and with a vial of the external layer. The heat flux for each slice is designed, respectively, as $\dot{Q}_2$ and $\dot{Q}_5$. As an example, by focusing on the slice 5 of the central vial, it exchanges heat only with the slice 6 of the vial of the external layer (being at different temperatures), while the net heat flux with the slice 1 of the other vial of the central layer is 0 (being at the same temperature). Therefore, the amount of heat flux for slices 2 and 5 is half that exchanged by slices 1 and 6. This finding is helpful for the evaluation of each contribution in the followings and explains the presence of the multiplicative factor "1/2" in the Eq. (12) reported below. Moreover, since the two contribution (slice 2 and 5) are equal between each other, the total heat flux is given by $2\dot{Q}_2$.

All these findings are useful to explicit the contribution of vial-to-vial heat flux, $\dot{Q}_{LAT}$, given by the sum of the contributions of the six slices:

$$\dot{Q}_{LAT} = \sum_{i=1}^{6} \dot{Q}_i = 2\dot{Q}_1 + 2\dot{Q}_2 \tag{10}$$

The contribution of each slice can be expressed as the product between the vial-to-vial heat transfer coefficient, K_{12}, the corresponding exchange area, A_{12}, and the driving force, so the temperature difference between the two layers:

$$\dot{Q}_1 = K_{12} A_{12} \left(\bar{T}_1 - \bar{T}_2 \right) = K_{12}^* \left(\bar{T}_1 - \bar{T}_2 \right) \tag{11}$$

$$\dot{Q}_2 = \frac{1}{2} K_{12} A_{12} \left(\bar{T}_1 - \bar{T}_2 \right) = \frac{1}{2} K_{12}^* \left(\bar{T}_1 - \bar{T}_2 \right) \tag{12}$$

It may be highlighted that the vial-to-vial heat transfer is due to several mechanisms, i.e. contact,

radiation and conduction in the gas, in a way similar to that occurring from the shelf to the product in the vial. This motivates the assumption of a linear driving force (taking also into account that the Stephan Boltzmann law may be approximated by a liner equation in case of low temperature difference). The evaluation of the exchange area is difficult, therefore it is convenient to use the effective heat exchange coefficient, K_{12}^{*}, given by the product between the vial-to-vial heat transfer coefficient and the area itself. The presence of the multiplicative factor "1/2" was discussed before. By substituting Eq. (11) and Eq. (12) in Eq. (10) it is possible to get:

$$\dot{Q}_{LAT} = \sum_{i=1}^{6} \dot{Q}_i = 3K_{12}^{*}\left(\overline{T}_1 - \overline{T}_2\right) \tag{13}$$

It should be highlighted that the perfectly central vial (indicated by the label "TP5" in Figure 1a) is surrounded by vials at the same temperature, thus the contribution $\dot{Q}_{LAT}$ is equal to 0 (the same consideration is valid for the seven central vials of the arrangement 2R in Fig. 1d). In other words, the term $\dot{Q}_{LAT}$ has to be multiplied by the number of central vials directly in contact with the external ones. Depending on the arrangement used, and as it is clearly visible in Fig. 1a and 1d, this multiplicative factor resulted equal to 6 (for 6R vials) or to 12 (for 2R vials).

The last contribution of heat in Figure 2 is given by the amount of heat that the external layer receives from the ring, being in direct contact with it, expressed by Eq. (14):

$$Q_{LyoSim} = K_L A_L \int_0^{\Delta t} \left(T_L - \overline{T}_1\right) dt \tag{14}$$

where K_L is the heat transfer coefficient between the external layer and LyoSim® and A_L is the corresponding exchange area. The temperature of fluid flowing into the ring is reported as T_L. All the other parameters are described above. The heat flux from the ring is obtained by dividing Q_{LyoSim} by Δt, as in the previous cases.

The various heat fluxes highlighted in Figure 2 for the layer 2 of vials, i.e. the central ones, are thus summarized in the following:

409 $$\dot{Q}_{base,int} = \frac{N_{int} K_v^* \int_0^t \left(T_S - \overline{T}_2\right) dt}{\Delta t},\ \dot{Q}_{LAT} = 3K_{12}^* \left(\overline{T}_1 - \overline{T}_2\right),\ \ \dot{Q}_{subl,int} = \frac{N_{int} \Delta H_s \overline{\Delta m_2}}{\Delta t} \quad (15)$$

410 and the corresponding amount of heat transferred during the test are summarized in the following:

411 $$Q_{base,int} = N_{int} K_v^* \int_0^t \left(T_S - \overline{T}_2\right) dt,\ Q_{LAT} = 3K_{12}^* \int_0^{\Delta t} \left(\overline{T}_1 - \overline{T}_2\right) dt,\ \ Q_{subl,int} = N_{int} \Delta H_s \overline{\Delta m_2} \quad (16)$$

412 One of the aims of the present paper is to estimate K_v starting from the experimental data of the
413 MicroFD® and compare it with that obtained from the REVO® freeze-dryer to validate the method.
414 For the calculations of all the heat fluxes, two parameters are unknown: K_v^* (equal to the product
415 between $A_{v,b}$ and K_v) and K_{12}^*, being all the temperatures and weight loss measured. The global energy
416 balance at the inner layer allows to find the relationship between K_v^* and K_{12}^*:

417 $$N_{int} Q_{base,int} + N_{LAT} Q_{LAT} = N_{int} Q_{subl,int} + N_{int} Q_{ACC} \quad (17)$$

418 where $Q_{base,int}$, Q_{LAT} and $Q_{subl,int}$ are shown in Eq. (16). The term N_{LAT} represents the number of vials
419 directly in contact with the external layer in the two arrangements, 6R and 2R. The values are clearly
420 visible in Fig. 1a and 1b and are, respectively, equal to "6" and "12". Besides, it may be convenient
421 to define the integrals appearing in Eq. (16) in a generic way by Eq. (18):

422 $$I_{xy} = \int_0^{\Delta t} \left(T_x - T_y\right) dt \quad (18)$$

423 Their values are known, as they just involve temperature measurements. By substituting each term in
424 Eq. (17), Equation (19) is thus obtained:

425 $$N_{int} K_v^* I_{S2} + 3N_{LAT} K_{12}^* I_{12} = N_{int} \Delta H_S \overline{\Delta m_2} + N_{int} Q_{ACC} \quad (19)$$

426 and the coefficient K_{12}^* may be expressed as a function of known or measured variables, and of the
427 only desired unknown (K_v^*):

428 $$K_{12}^* = \frac{N_{int} \Delta H_S \overline{\Delta m_2} + N_{int} Q_{ACC} - N_{int} K_v^* I_{S2}}{3N_{LAT} I_{12}} \quad (20)$$

Q_{ACC} is the heat accumulation term, that is explicitly taken into account in eq. (17) to increase the accuracy of the method, taking also into account the duration of the test that may be slow and, thus, the role of the heat accumulation occurring in the first part may be not negligible. The accumulation term may be calculated from the following equation:

$$Q_{ACC} = \int_0^{\Delta t} \left[\frac{d}{dt} \left(m_{ice} c_p T_{ice} \right) \right] dt \tag{21}$$

It is convenient to express the mass of ice as a function of the thickness of the ice. For each time interval, the mass of ice and its thickness at the generic instant *t* can be calculated by Eq. (22) and (23):

$$m_{ice}(t) = m_{ice}(0) - \int_0^t J_w dt \tag{22}$$

$$L_{ice}(t) = \frac{m_{ice}(t)}{\rho_{ice} A_{v,i}} \tag{23}$$

being J_w the sublimation flux. By expressing the mass of ice as a function of its thickness, the accumulation term becomes:

$$\begin{aligned} Q_{ACC} &= \int_0^{\Delta t} \left[\frac{d}{dt} \left(m_{ice} c_p T_{ice} \right) \right] dt = c_p \int_0^{\Delta t} \left[m_{ice} \frac{d}{dt} \left(T_{ice} \right) \right] dt + c_p \int_0^{\Delta t} T_{ice} \left[\frac{d}{dt} \left(m_{ice} \right) \right] dt = \\ &= c_p \rho_{ice} A_{v,i} \int_0^{\Delta t} L_{ice} dT_{ice} + c_p \rho_{ice} A_{v,i} \int_0^{\Delta t} T_{ice} dL_{ice} \end{aligned} \tag{24}$$

In order to know Q_{ACC} it is needed to evaluate L_{ice} vs. time, in such a way that the two integrals may be calculated. The calculation of L_{ice} is based on Eqs. (22) and (23), provided that J_w is known. Due to the high conductivity of ice, the content in each vial was assumed, in this step, to be isothermal and at a temperature equal to that measured by the thermocouple. So, it is possible to express the sublimation flux as:

$$J_w = KK \left(p_{w,i} - p_{w,c} \right) \tag{25}$$

as it is directly proportional to the difference between the vapor pressure at the interface of sublimation, $p_{w,i}$, and that in the drying chamber, $p_{w,c}$, that is coincident with the total pressure in the

chamber, P_c, since the gas in the chamber is about 100% water vapor. *KK* takes into account all the mass transfer resistances from the interface of sublimation to the drying chamber, mainly the stopper. The water vapor pressure at the interface of sublimation depends on the temperature and can be calculated by the Goff-Gratch relationship shown in Eq. (26):

$$p_{w,i} = 10^{-9.09718\left(\frac{273.16}{T_i}-1\right)-3.56654\log_{10}\left(\frac{273.16}{T_i}\right)+0.876793\left(1-\frac{T_i}{273.16}\right)+\log_{10}6.1071} \quad (26)$$

The sublimated mass, measured during the test, is found by integrating Eq. (26):

$$m_{sub} = \int_0^{\Delta t} KK\left(p_{w,i} - p_{w,c}\right)dt \quad (27)$$

KK is considered as a constant since the variations of temperature and of the sublimation flux are negligible in the operating conditions considered in the present work. It can be evaluated from Eq. (27) by considering the measured variations in mass (at the end of the gravimetric test) and integrating the driving force over time, obtaining Eq. (27):

$$KK = \frac{\overline{\Delta m_2}}{\int_0^{\Delta t}\left(p_{w,i} - p_{w,c}\right)dt} \quad (28)$$

KK may be thus calculated at the end of the test, as all the variables and parameters needed in Eq. (28) are either measured or known, and this allows calculating, at each time step J_w, through Eq. (25) , and from J_w it becomes possible to calculate, at each time step, L_{ice} through Eqs. (22) and (23), and, finally, Q_{ACC}, through Eq. (24). By this way, K_{12}^* may be expressed through Eq. (20) as a known function of K_v^*.

The last step of the algorithm is the calculation of the temperature evolution in each vial of the central layer during the gravimetric step through a mathematical model. The two differential equations to be solved are the mass balance (Eq. (29)) and the energy balance (Eq. (30)):

$$\frac{dL_{ice}}{dt} = -\frac{KK\left(p_{w,i} - p_{w,c}\right)}{\rho_{ice}A_{v,i}} \quad (29)$$

$$\rho_{ice} c_p A_{v,i} \left(L_{ice} \frac{dT_{ice}}{dt} + T_{ice} \frac{dL_{ice}}{dt} \right) = K_v^* \left(T_S - T_{ice} \right) + 3K_{12}^* \left(T_1 - T_{ice} \right) - \Delta H_s J_w \quad (30)$$

By substituting Eq. (29) in Eq. (30), the result becomes:

$$\frac{dT_{ice}}{dt} = \frac{1}{\rho_{ice} c_p A_{v,i} L_{ice}} \left[K_v^* \left(T_S - T_{ice} \right) + 3K_{12}^* \left(T_1 - T_{ice} \right) - \Delta H_s KK \left(p_{w,i} - p_{w,c} \right) + c_p T_{ice} KK \left(p_{w,i} - p_{w,c} \right) \right] \quad (31)$$

By using this approach only one parameter, K_v^*, remains unknown in Eq. (31). Therefore, it is possible to find it using a "best-fit" procedure. In other words, the value of K_v (by explicating $K_v^* = K_v A_{v,b}$) that minimizes the mean square deviation between measured and calculated ice temperature was calculated. For this purpose, a MATLAB script was written using the function "*fminsearch*". This function required an initial estimate for K_v^* (the stationary value of K_v^* was used in the present work as initial estimate calculated using the stationary energy balance by considering the asymptotic value of the temperature profiles). However, it was derived that the result was independent on the value used as the initial estimate of K_v^*, thus ensuring the robustness of the algorithm. The differential equation (Eq. (31)) was solved using "*ode15s"* solver for each time interval. As a result, the calculated ice temperature and the thickness of the dried cake as a function of time were obtained and, obviously, the value of the heat transfer coefficient, K_v, in the MicroFD® freeze-dryer.

2.3.3 R_p Calculation

As a consequence of the sublimation of ice, a solid porous structure is obtained, called cake. The water vapor must pass through the porous cake, leaves the dried layer and escapes from the vial. The sublimation flux, J_w, is expressed as a function of the driving force as reported in Eq. (32):

$$J_w = \frac{1}{R_p} \left(p_{w,i} - p_{w,c} \right) \quad (32)$$

The resistance of the dried product to vapor flow is defined as R_p. The mass transfer takes place under

494 rarefied gas conditions. Therefore, it must be taken into account that the fluid cannot be considered
495 as a continuous medium, where interactions between molecules predominate over interactions
496 between the molecules and the solid walls of the container. In this case, interactions between gas
497 molecules and the solid walls are predominant. Then, the sublimation flux, due to the Knudsen
498 diffusion, is given by Eq. (33):

499 $$J_w = \frac{D_e}{L_{dried}}\left(c_{w,i} - c_{w,c}\right) \quad (33)$$

500 where $c_{w,i}$ and $c_{w,c}$ are, respectively, the water vapor concentrations at the interface of sublimation
501 and in the drying chamber and D_e is the effective diffusivity. Usually, eq. (33) is written as eq. (32),
502 by expressing the driving force in terms of difference of vapour pressure, and introducing the
503 resistance of the dried product, R_p. Using the approach presented in previous papers[29], it is possible
504 to assess that R_p is a function of the dried layer thickness (L_{dried}), and the following equation is the
505 reference one:

506 $$R_p = R_{p,0} + \frac{AL_{dried}}{1 + BL_{dried}} \quad (34)$$

507 While $R_{p,0}$ is a fitting parameter used to point out the existence of a top layer characterized by a
508 significantly higher resistance to vapor flow than in the rest of the cake, the two parameters A and B
509 may be related to cake structure, and, in particular, to the distribution of pore size in the cake. A linear
510 dependence of mean pore radius (r_e) on cake thickness (and tortuosity, τ) may be assumed[29]:

511 $$\frac{r_e}{\tau} = a_0 + a_1 L_{dried}$$

512 and, thus, it is possible to get:

513 $$A = \frac{RT_{dried}^{0.5}}{a_0 M_w K \varepsilon},\ B = \frac{a_1}{a_0} \quad (35)$$

514 where ε is the void fraction or porosity (difference between 1 and the percentage of solute), K is equal
515 to $22.9\frac{m}{s \cdot K^{0.5}}$, M_w is the molecular weight of water, R is the ideal gas constant and T_{dried} is the
516 temperature of the dried product, considered equal to T_i.[29]
517 To describe the evolution of the thickness of the dried cake (and, thus, also the drying time) and the
518 product temperature profiles over the time, a Matlab script was used, simulating the freeze-drying

519 process, by solving Eq. (36), mass balance for the dried layer, and Eq. (37), heat balance for the
520 frozen, layer:

521 $$\frac{dL_{dried}}{dt} = -\frac{1}{\rho_{frozen} - \rho_{dried}} J_w \tag{36}$$

522 $$T_B = T_S - \frac{1}{K_v}\left(\frac{1}{K_v} + \frac{L_{frozen}}{\lambda_{frozen}}\right)^{-1}\left(T_S - T_i\right) \tag{37}$$

523 where ρ_{frozen} and ρ_{dried} are, respectively, the density of the frozen product and that of the dried cake.
524 The parameter λ_{frozen} represents the thermal conductivity of the frozen product and it was equal to
525 $2.56\ \frac{J}{m \cdot s \cdot K}$. By combining eq. (1) and eq. (32) into the heat balance at the interface of sublimation:

526 $$J_q A_{w,b} = \Delta H_S J_w A_{v,i} \tag{38}$$

527 the instantaneous resistance to vapor flow, R_p, was derived as:

528 $$R_p = \frac{\left(p_{w,i} - p_{w,c}\right) A_{v,i} \Delta H_S}{K_v \left(T_S - T_B\right) A_{v,c}} \tag{39}$$

529 In order to obtain the instantaneous thickness of the dried cake, it is necessary to calculate the amount
530 of sublimated water from the beginning of the primary drying (indicated as 0) to the generic time
531 instant t^*:

532 $$m_w^* = A_{v,i} \int_0^{t^*} J_w dt \tag{40}$$

533 The instant "0" was derived by looking for the condition: $p_{w,i} > P_c$. By considering the porosity of the
534 matrix, Eq. (23) becomes:

535 $$L_{dried} = \frac{m_w^*}{\rho_{frozen} \varepsilon A_{v,i}} \tag{41}$$

536 By plotting R_p as a function of L_{dried}, instant by instant, the desired curve is obtained. As deeply
537 discussed in Section 2, it is possible to traceback to Eq. (34). The parameters a_0 and a_1 are function
538 of A and B, determined by minimizing the mean square deviation between experimental and
539 theoretical values using the non-linear GRG method implemented in the Excel solver.

3. Results and Discussions

3.1 Study of the heat transfer coefficient

The first part of the study was focused on the development and validation of the model able to find K_v starting from the experimental data obtained in the gravimetric test carried out in the small-scale freeze-dryer. So, as a first step we wanted to evaluate how close the values of K_v obtained in the small-scale freeze-dryer were to the ones obtained in a larger unit.

The experimental temperature profiles for the 2R vials, in MicroFD® and in REVO® freeze-dryers, are reported in Figure 4 for different values of chamber pressure during the sublimation step (6.7, 13.3 and 26.7 Pa) of the gravimetric test. In the first column, the results obtained in the MicroFD® can be observed, while in the second column the ones in the REVO® device are given.

Three thermocouples (TP1, TP2 and TP1), measuring the temperature of the central vials, were used in the REVO® equipment. Instead, in the MicroFD® device five thermocouples were used: TP3 and TP7 refers to the edge vials, while TP4, TP5 and TP6 to the central ones. Some signals were not reported here since they were considered unreliable, very different from the others. This could be due to a placement error, so the thermocouple was not in perfect contact with the bottom of the vial, or to the loss of contact between the thermocouple and the ice during the test. A close inspection of Figure 4 indicates that, for each graph, the different signals of the thermocouples are very similar (at the same pressure value, but in the two different scales). The difference is about ±2°C. Evidence for this is visible by comparing Fig. 4a and 4d, where it is possible to notice that the asymptotic product temperatures range from -41°C to -39°C. The same can be observed for the other two values of pressure: 13.3 and 26.7 Pa. Moreover, all these considerations are valid for the case of 6R vials, whose graphs are reported in Fig. S1 in the Supplementary Material. For the calculation of the heat transfer coefficient, a unique temperature profile for the external layer and one for the internal layer is required. Therefore, in the case of external layer the average temperature profile between the TP3 and TP7 was selected; while for the internal layer the average temperature profile among TP4, TP5 and

566 TP7 was used.

567 Figure 5 illustrates the heat transfer coefficient obtained as a function of pressure for both freeze-
568 dryers and type of vials (2R or 6R). As it was expected, as chamber pressure increases, the heat
569 transfer coefficient increases. In fact, the increase in pressure implies an increase in the thermal
570 conductivity of the gas in the gap between the bottom of the vial and the shelf surface. Lines were
571 found using Eq. (42):

572 $$K_v = C + \frac{DP_c}{1 + EP_c} \tag{42}$$

573 The fitting parameters, *C*, *D* and *E* were calculated by minimizing the mean square deviation between
574 the experimental and the theoretical values.

575 Excellent results were achieved in terms of comparison of K_v values for the MicroFD® freeze-dryer
576 and the REVO® one. In fact, as it is shown in Figure 5a and 5b, the two curves (the solid and the
577 dashed line) resulted very close for both 2R and 6R vials type. This finding was evidence of the
578 accuracy of the developed algorithm. The mean values of the heat transfer coefficient and the relative
579 error was calculated and reported in Table 1. According to the data shown in Table 1, a relative
580 maximum error of 7% was reached, in the worst case, that is the one at 13.3 Pa using 2R vials. It is
581 considered as absolutely acceptable, considering that in gravimetric tests a standard deviation of
582 around 10% is not unusual.

583 Table 1 shows also the values of K_v obtained for central vials, the ones of interest in this study,
584 obtained just considering their weight loss, the heat of sublimation and the temperature difference
585 between the shelf and the product, i.e. the usual approach that neglects the contribution of the lateral
586 flux to the heat balance in the vial. It appears that this value ($K_{v,MicroFD,bottom}$) is quite different from
587 the value of $K_{v,MicroFD}$ obtained through the previously described algorithm and, what is more
588 important, from the value of $K_{v,REVO}$. This is another evidence of necessity of including the lateral
589 heat flux in the heat balance for the gravimetric test carried out in MicroFD®. The values of weight
590 loss at the basis of the calculations shown in Table 1 are given in the supplementary materials /Table

591 S1 and S2).

592 By exploiting the K_v values obtained with the Matlab algorithm in the first part of the study, all the
593 heat fluxes were calculated and reported in Table 2. According to the data reported in Table 2, the
594 heat fluxes of sublimation, $\dot{Q}_{subl,int}$ and $\dot{Q}_{subl,ext}$, increases as the pressure increases for both kind of
595 vials (2R or 6R). This finding was expected, since, as underlined before, the thermal conductivity of
596 the gas increases and, thus, the heat flux to the product in the vial that, finally, results in ice
597 sublimation. The same trend was found for the heat fluxes received from the product by the shelf,
598 $\dot{Q}_{base,int}$ and $\dot{Q}_{base,ext}$. Moreover, for the 2R vials, the trend of inter-layer heat flux, $\dot{Q}_{LAT}$, is
599 monotonically increasing with pressure, as it could be expected. No specific trend was found for the
600 heat flux received by the external layer from the ring, $\dot{Q}_{LyoSim}$. For each layer, it was possible to relate
601 each flow to the total heat flux. Specifically, for the internal layer the percentage of heat received by
602 the surrounding vials and the one from the shelf was calculated, by considering only the sublimation
603 term as heat output, by Eq. (43). For the external layer two different incoming flows were present in
604 the system: the one coming from the shelf and the one from LyoSim®. The total amount of heat
605 leaving the outer layer is given by the sum of the sublimation heat and the vial-to-vial term, as
606 reported in Eq. (44). Therefore, the following percentages could be calculated:

$$\%\ lat = \frac{\dot{Q}_{LAT}}{\dot{Q}_{subl,int}}, \qquad \%\ base,int = \frac{\dot{Q}_{base,int}}{\dot{Q}_{subl,int}} \tag{43}$$

$$\%\ LyoSim = \frac{\dot{Q}_{LyoSim}}{\dot{Q}_{subl,ext} + \dot{Q}_{LAT}}, \qquad \%\ base,ext = \frac{\dot{Q}_{base,ext}}{\dot{Q}_{subl,ext} + \dot{Q}_{LAT}} \tag{44}$$

607 Figure 6 provides a clear visualization of the obtained results. It demonstrates that most of the
608 sublimation heat of the inner layer is provided by the shelf and less than 10%, for all three pressure
609 values, is supplied by the surrounding vials. As an example, by focusing at 6.7 Pa, the percentage
610 provided by the shelf is equal to 99% against the 1% provided by the surrounding vials. The maximum
611 value for this term is reached at the highest pressure value, 26.7 Pa, where they are respectively equal
612 to 91% and 9%. Therefore, the increasing trend for the vial-to-vial heat flux, noticed in Table 2, is

here confirmed and clearly visible. Instead, the overall heat entering the outer layer comes equally from the shelf and the LyoSim® for all the three different values of pressure. As a matter of fact, by focusing for example at 13.3 Pa, the percentage of heat provided by LyoSim® resulted equal to 42.11% against the 57.89% provided by the shelf. The trends for the 6R vials arrangement are reported in Figure S2 of the Supplementary Material. In Figure S3 the trends of the heat fluxes as a function of pressure are also reported.

In conclusion, the main achievements of the study are the followings:

- A vial-to-vial heat term must be introduced in the mathematical model to take into account the heat contribution from the edge vials as LyoSim® temperature is not optimized to get a uniform batch (aiming to reduce the experimental effort). Thanks to this term, it was possible to distinguish between the heat due to the exchange with the shelf and that exchanged with the other vials and/or the ring.
- The developed algorithm is able to accurately estimate K_v in a pilot-scale freeze-dryer starting from the experimental data of the MicroFD® freeze-dryer. In fact, the obtained values in the MicroFD® were close to the ones obtained in a larger freeze-dryer, thus allowing for the reduction of the experimental effort, essential in the current methods to reach the optimal value for the offset temperature. Therefore, coupling of MicroFD® experimental tests with a mathematical model could be a suitable solution to facilitate and speed up the design of a freeze-drying cycle for a larger scale unit.

3.2 Study of the resistance of the dried cake to vapor flow

To design a freeze-drying cycle it is extremely important to know the drying time and the maximum product temperature. Therefore, beside K_v, the value of R_p is necessary to enable mathematical simulation of the process. The freezing conditions affect the porosity of the matrix, thus the R_p value, as they are responsible for the number and the size of ice crystals.[30] For a given product, and if the freezing conditions are the same in both the small-scale and large-scale freeze-dryer, and the same

639 filling conditions are used, it is expected that the same values of R_p are obtained. Therefore, it is
640 reasonable to expect that the type of vial (2R or 6R) does not affect the R_p vs L_{dried} curve. The vapor
641 flow resistance depends only on the thickness of the dried layer through the Eq. (36). The parameters
642 $R_{p,0}$, A and B can be found by minimizing the error between the experimental values and the
643 theoretical ones. The parameter R_p was found through experimental tests directly exploiting the
644 product temperature profiles and using the K_v value found by the algorithm (the one obtained with
645 the gravimetric test in the MicroFD®). As described in Section 2, all the experimental tests were
646 carried out at 13.3 Pa and by setting T_S to -10°C during the primary stage. The LyoSim® offset was
647 set to -3°C with respect to the mean product temperature, on the basis of previous studies, although
648 different values can be used.
649 The mass transfer experimental parameters obtained for the 13.3 Pa pressure are reported in Table 3.
650 The experimental curves relating r_e/τ as a function of the thickness of the dried cake are reported in
651 Figure 7. The three curves are similar, taking also into account the uncertainty of the approach, as it
652 was expected according to the data reported in Table 3, but there is a discrepancy among them. It is
653 therefore important to deepen the study focusing on the influence of this difference on the main
654 features of the freeze-drying process (product temperature and drying time).
655 Therefore, the aim of this part of the study was to investigate the influence of the R_p parameters on
656 product temperature profiles and the duration of the primary drying. For this purpose, it is possible to
657 focus on a specific curve, for example the one of the 2R vials in the MicroFD® (dash-dot line in Fig.
658 7) by considering the R_p parameter as the same for all the curves. In other words, the experimental
659 parameters derived for 2R vials (reported in Table 3) were used for the simulation of what occurs in
660 6R vials using a Matlab script that simulates the dynamic of the freeze-drying process. For each
661 simulation, the previously determined K_v parameter by gravimetric tests was used according to the
662 case (type of vial and equipment). The product temperature profiles and the time required to complete
663 the primary drying were calculated and compared with the experimental values found for 6R vials,
664 both in MicroFD® and REVO® freeze-dryers. In such a way, it was possible to assess the reliability

665 of the model parameters. Specifically, the influence of the small initial difference in R_P values
666 (between 2R and 6R vials) on the freeze-drying process was evaluated.
667 Figure 8 summarizes the results obtained in the MicroFD® and REVO® devices for a 5% w/w sucrose
668 solution processed in the same operating conditions but in different type of vials (2R and 6R). The
669 experimental ratio between the Pirani and the Baratron sensor signals can be used to assess the drying
670 time, as reported in Fig. 8a. As a result of simulation, instead, it was possible to use the trend of the
671 dried cake thickness as a function of time: the drying time was reached when the thickness of the
672 frozen layer was equal to 0, as shown in Fig. 8b. The experimental identification of the ending point
673 using the pressure ratio is really difficult as it refers to the concentration of the water vapor in the
674 dryer chamber and not to the amount of ice in the vial, although, obviously, the presence of ice in the
675 vial and, thus, the sublimation flux affect the composition in the chamber. In Fig. 8a, a constant trend
676 is observed during the primary drying. When ice sublimation is completed, the curve decreases
677 rapidly until it reaches an asymptotic limit value. The starting point in the curve is almost 1.7, since
678 the Pirani vacuum gauge measures the thermal conductivity of the gas in the drying chamber, so it
679 reads about 60% higher than the Baratron manometer. In fact, the thermal conductivity of water vapor
680 is almost 1.6 times the thermal conductivity of nitrogen. When the gas composition inside the
681 chamber is changing from water vapor to nitrogen, index of sublimation occurred, the ratio
682 Pirani/Baratron starts to decrease. The point at which this decrease begins is called “onset”, while the
683 point where the lower asymptote is reached is the “offset”. It was reported that onset, offset and mid
684 points may be representative of drying time.[23] In this framework, model calculation of drying time
685 (i.e. the point when frozen layer thickness approaches zero) may be considered validated it is between
686 the onset and the offset, as it occurs in this case. By considering the onset point, for the 2R vials
687 (black solid line), the experimental drying time is about 721 minutes, while the calculated one is 705
688 minutes. The relative error is lower than 5% (2.2% to be precise). For the 6R vials in the MicroFD®
689 freeze-dryer (light gray line), the experimental drying time is 1006 minutes, while the calculated one
690 is 1038 minutes, leading to a relative error lower than 5% (3.2% to be precise). Lastly, for the 6R

691 vials in the REVO® device (dark grey line), the values are respectively equal to 903 and 979 minutes,
692 leading to a relative error lower than 10% (8.4% to be precise). In the evaluation of the results, it is
693 important to stress that the experimental drying time values are subjected to a non-negligible
694 uncertainty, since they are determined graphically, and the curves are very noisy.
695 Figure 9 illustrates the product temperature profiles in three different situations by considering the
696 value of pressure equal to 13.3 Pa. The solid black line represents the experimental profile evaluated
697 in the REVO® equipment using the 6R vials arrangement. The dashed black line represents the
698 calculated temperature profile through mathematical simulation of the process by using the
699 experimental R_p value derived for the 6R vials in MicroFD® (see Table 3 for the values). The last
700 curve, the grey one, instead, represents the calculated temperature profile through mathematical
701 simulation of the process by using the experimental R_p value derived for the 2R vials MicroFD®
702 (values reported in Table 3). Again, the purpose is always the same: to test the reliability of the model
703 parameters (K_v and R_p) obtained in MicroFD®.
704 As it is clearly visible in Fig. 9, the three curves are almost overlapping, demonstrating that the
705 differences in fitted parameters ($R_{p,0}$, A and B) do not have a large impact on modelling results. In
706 fact, the trends obtained differ by approximately 1°C, that is the uncertainty of a T-type thermocouple.
707 As it was expected, the type of vial does not influence the R_p value. In fact, the product temperature
708 trend is pretty the same whether we use experimental R_p value found for 2R vials or 6R vials to
709 simulate the process dynamic. This was a great achievement, since it is possible to use the MicroFD®,
710 for a given product, to obtain the model parameters (K_v and R_p) of a larger freeze-dryer, saving time
711 and materials. Moreover, it is also possible to correctly and accurately simulate the dynamics of a
712 larger-equipment, so the REVO® device, using the model parameters found in the Micro-FD®. Figure
713 S4 of the Supplementary Materials provides further validation.
714 This result was largely expected. In fact, resistance of the dried cake is dependent on the size of the
715 pores that, in turn, is dependent on the size of the ice crystals. Being freezing a stochastic phenomenon
716 in both freeze-dryers (no controlled nucleation has been used either in MicroFD® or in larger units,

717 at industrial scale, freezing is almost always carried out in an uncontrolled way), the structure of the
718 dried cake is not expected to be different, obviously in case no shrinkage or collapse occurs (but this
719 is the target of the step of process design/optimization). Surely the way of heat transfer from the
720 freeze-dryer to the product in the vial is different and, thus, the product temperature and the drying
721 time, but R_p should not be affected by the equipment used, and results shown in Figure 9 agree with
722 this.
723 It has to be highlighted that when using MicroFD® for process development the optimal approach is
724 to use here the same type of vial that will then used in the larger unit, thus minimizing scale-up issues
725 in the step of process transfer. Anyway, in case this is not possible, either because a "special" type of
726 vial is planned to be used and, thus, the LyoSim® ring is not readily available, or the type of vial (and
727 manufacturer) is not yet identified, then MicroFD® may in any case be used to evaluate R_p vs. L_{dried},
728 as cake resistance is not a function of vial size and type, but just of product structure.
729
730 **4. Conclusions**
731 In the present paper a novel model-based approach for the design of the primary drying stage starting
732 from the experimental data of a small-scale freeze-dryer (MicroFD®) was shown. The main aim was
733 to investigate if the small-scale freeze-dryer could be used for process investigation and development,
734 facilitating and speeding up the scale-up procedures. Here, an effective procedure for scale-up has
735 been proposed, saving time and material with respect to the current methods.
736 We demonstrated that it is possible to couple the MicroFD® with a mathematical model to accurately
737 calculate K_v through gravimetric tests. The obtained values resulted very similar to the one obtained
738 in the larger freeze-dryer (REVO®). Moreover, the use of the algorithm, by including the vial-to-vial
739 heat term, allows for a reduction in the experimental effort required to do the tests. In fact, it allows
740 to overcome the problem of finding the optimal ring temperature to achieve homogeneous conditions
741 in the batch. Moreover, it is necessary to stress the importance of the inter-layer heat term to take into
742 account the presence of the ring and better simulate the dynamics of the central vials in the MicroFD®.

In the second part of the study, a very good agreement was reached for R_p. We demonstrated that it is possible to study a given formulation, in a certain type of vial (2R or 6R in the present case), in the MicroFD® to simulate and predict its behavior (in terms of drying time and temperature profile) in a larger-scale freeze-dryer (REVO®). An evidence for this was given by the comparison of the experimental and calculated product temperature profiles. According to the results obtained, it is indifferent to use 2R or 6R vials to study the evolution of product temperature. This is a valuable result, since the R_p parameters for 6R vials can be used to simulate the process of the 2R vials in the REVO® equipment (using the proper K_v value found by gravimetric test). Again, the presented strategy allows for the development of freeze-drying cycles, representative of larger scales, on the MicroFD®, leading to save time and materials.

To summarize, the steps to be followed for obtaining efficient results are here reported:

1) Do the gravimetric test in the MicroFD® equipment to calculate K_v using the mathematical algorithm proposed in this paper. Since K_v does not depend on the product, you can do this step using only water;
2) Do another test in the same equipment, the MicroFD®, using the product of interest, to calculate the experimental curve R_p vs L_{dried}, using the same filling procedure and the same freezing protocol that will be used in the larger scale. In this test it is required to measure the product temperature profile, and to operate at the same pressure and with the same type of vial used in the previous step as it is required to know K_v;
3) Use the K_v found at step 1) and R_p found at step 2) to simulate the process dynamics in a different unit, so calculating the product temperature profiles and the time required to complete the primary drying.

At this point, a test may be carried out in the larger unit for validation purposes. It is always necessary to carry out at least one test in the larger unit, quite often indicated as “engineering run”, to validate the cycle developed at smaller scale. In some cases, in fact, it may observed a difference even in the value of K_v for the central vial, due to differences in the roughness of the shelf surface, or in the

769 performance of the heating system. This situation is not very common, but it may occur, and, in this
770 case, the traditional approach, based on the thermal characterization of the large freeze-dryer and on
771 the optimization of the temperature of the heating ring is unavoidable if a true replication of the
772 heating conditions in the two units is desired. In this case, the results obtained following the algorithm
773 proposed in this paper have to be regarded as a first guess approach.
774
775 **Acknowledgments**
776 The authors would like to acknowledge Millrock Technology Inc., for the financial support and the
777 useful suggestions for the use of the device. Valuable contribution of Andrea Lupano (Politecnico di
778 Torino) to the experimental investigation is gratefully acknowledged.
779
780 **Declaration of interest: Role of the funding source**
781 Millrock Technology Inc. has supported the study by loaning the MicroFD® used in this study to the
782 research group of the Politecnico di Torino and by helping the researchers to solve practical issues
783 related to the experimental investigation.

References

1. Wang, B.S. & Pikal, M. J. *Stabilization of lyophilized pharmaceuticals by process optimization: Challenges and opportunities*. Am. Pharm. Rev. 2012; 82-89.
2. Fissore, D. *Freeze Drying of Pharmaceuticals*. Encyclopedia of Pharmaceutical Science and Technology. Taylor and Francis: New York, 2013; 1723-1737. http://dx.doi.org/10.1081/E-EPT4-120050278
3. Bellows, R.J. & King, C.J. *Freeze-drying of aqueous solutions: maximum allowable operating temperature.* Cryobiology. 1972; 9(6): 559-561. https://doi.org/10.1016/0011-2240(72)90179-4
4. Barresi, A. A.; Ghio, S.; Fissore, D.; & Pisano, R. *Freeze drying of pharmaceutical excipients close to collapse temperature: Influence of the process conditions on process time and product quality*. Dry. Technol. 2009**;** 27(6): 805–816**.** https://doi.org/10.1080/07373930902901646
5. Rathore, A.S. & Winkle, H. *Quality by design for biopharmaceuticals*. Nat. Biotechnol. 2009; 1: 26-34. https://doi.org/10.1038/nbt0109-26
6. Giordano, A., Barresi, A.A. & Fissore D. *On the use of mathematical models to build the design space for the primary drying phase of a pharmaceutical lyophilization process.* J. Pharm. Sci. 2011;100(1): 311-324. https://doi.org/10.1002/jps.22264
7. Fissore, D., Pisano, R., & Barresi, A.A. *Advanced approach to build the design space for the primary drying of a pharmaceutical freeze-drying process.* J. Pharm. Sci. 2011; 100(11):4922-4933. https://doi.org/10.1002/jps.22668
8. Koganti, V.R, Shalaev, E.Y., Berry, M.R., Osterberg, T., Youssef, M., Hiebert, D.N., Kanka, F.A., Nolan, M., Barrett, R., Scalzo, G., Fitzpatrick, G., Fitzgibbon, N., Luthra, S., & Zhang, L. *Investigation of design space for freeze-drying: Use of modeling for primary drying segment of a freeze-drying cycle.* AAPS PharmSciTech. 2011;12(3):854-861. https://doi.org/10.1208/s12249-011-9645-7
9. Fissore, D., Gallo, G., Ruggiero, A.E. & Thomson T.N. *On the use of a micro freeze-dryer*

for the investigation of the primary drying stage of a freeze-drying process. Eur. J. Pharm. Biopharm. 2019; 141: 121-129. https://doi.org/10.1016/j.ejpb.2019.05.019

10. Fissore, D. & Barresi, A. A. *Scale-up and process transfer of freeze-drying recipes*. Dry. Technol. 2011; 29(14): 1673-1684. https://doi.org/10.1080/07373937.2011.597059
11. Pisano, R., Fissore, D., & Barresi, A.A. *Heat transfer in freeze-drying apparatus*, in: M. A. Dos Santos Bernardes (Ed.), Heat Transfer; Intech, Rijeka, Croatia, 2011; 91-114. https://doi.org/10.1016/10.5772/23799
12. Pikal, M.J., Bogner, R.H., Mudhivarthi, V., Sharma, P., & Sane, P. *Freeze-drying process development and scale-up: scale-up of edge vial vs. center vial heat transfer coefficients, Kv.* J. Pharm. Res. 2016; 105:3363–43. https://doi.org/10.1016/j.xphs.2016.07.027
13. Moino, C., Bourlés, E., Pisano, R., & Scutellà, B. *In-line monitoring of the freeze-drying process by means of heat flux sensors.* Ind. Eng. Chem. Res. 2020; 60:9637-9645. https://doi.org/10.1021/acs.iecr.1c00536
14. Scutellà, B., Plana-Fattori, A., Passot, S., Bourlès, E., Fonseca, F., Flick, D., & Trelea, I.C. *3D mathematical modeling to understand atypical heat transfer observed in vial freeze-drying*. Appl. Therm. Eng. 2017; 12: 226-236. https://doi.org/10.1016/j.applthermaleng.2017.07.096
15. Thompson, T.N. & Fissore, D., *Use of a micro freeze-dryer for developing a freeze-drying process*. 2019. in "Freeze Drying of Pharmaceutical Products", (D. Fissore, R. Pisano and A. Barresi, Eds.) Chap. 7. CRC Press, Taylor & Francis Group, pp. 131-143. [ISBN: 978-0429-02207-4]
16. Matejčíková, A. Tichý, E. & Rajniakac P. Experimental investigation of inhomogeneities of primary drying during lyophilization: Impact of the vials packing density. J. Drug. Dev. Sci. Tech. 2022;74: 103550. https://doi.org/10.1016/j.jddst.2022.103550
17. Elhers, S., Schroeder, R. & Friess W. *Trouble with the neighbor during freeze-drying: Rivalry about energy*. J. Pharm. Sci. 2021; 110(3): 1219-1226.

https://doi.org/10.1016/j.xphs.2020.10.024

18. Scutellà, B., Passot, S. Bourlés, E., Fonseca, F. & Trélea, I.C. *How vial geometry variability influences heat transfer and product temperature during freeze-drying*. J. Pharm. Sci. 2016; 1-9. https://doi.org/10.1016/j.applthermaleng.2017.07.096
19. Obeidat, W.M., Bogner, R., Mudhivarthi, V., Sharma, P., & Sane, P. *Development of a mini-freeze dryer for material-sparing laboratory processing with representative temperature history*. AAPS PharmSciTech. 2018; 29:599-609. https://doi.org/10.1208/s12249-017-0871-5
20. Thompson, T.N., Wang, Q., & Reiter, C. *Developing transferable freeze-drying protocols using accuflux and a MicroFD.* Presentation given at Peptalk 2017, San Diego, USA. Available at: https://pharmahub.org/groups/lyo/tools. Accessed November 2022.
21. Goldman, J.M., Chen, X., Register, J.T., Nesarikar, V., Iyer, L., Wu, Y., Mugheirbi, N. & Rowe J. *Representative scale-down lyophilization cycle development using a seven-vial freeze-dryer (MicroFD®).* J. Pharm. Sci. 2019; 108(4): 486-1495. https://doi.org/10.1016/j.xphs.2018.11.018
22. Fissore, D., Harguindeguy, M., Velez Ramirez, D. & Thompson, T.N. *Development of freeze-drying cycles for pharmaceutical products using a micro freeze-dryer*. J. Pharm. Sci. 2020; 109: 797-806. https://doi.org/10.1016/j.xphs.2019.10.053
23. Patel, S.M., Doen, T. & Pikal, J.M. *Determination of end point of primary drying in freeze-drying process control*. AAPS PharmSciTech. 2010; 11: 73-84. https://doi.org/10.1021/10.1208/s12249-009-9362-7
24. Sadikoglu, H.; & Liapis, A.I. *Mathematical modelling of the primary and secondary drying stages of bulk solution freeze-drying in trays: Parameter estimation and model discrimination by comparison of theoretical results with experimental data.* Dry. Technol. 1997; 15: 791–810. https://doi.org/10.1080/07373939708917262
25. Gan, K.H.; Crosser, O.K.; Liapis, A.I.; & Bruttini, R. *Lyophilisation in vials on trays: Effects*

862 *of tray side.* Dry. Technol. 2005; 23: 341–363. https://doi.org/10.1081/DRT-200047671
863 26. Hottot, A.; Peczalski, R.; Vessot, S.; & Andrieu, J. *Freeze-drying of pharmaceutical proteins*
864 *in vials: Modeling of freezing and sublimation steps.* Dry. Technol. 2006; 24, 561–570.
865 https://doi.org/10.1080/07373930600626388
866 27. Velardi, S.A. & Barresi, A.A. *Development of simplified models for the freeze-drying process*
867 *and investigation of the optimal operating conditions.* Chem. Eng. Res. Des. 2008; 86(1):9-
868 22. https://doi.org/10.1016/J.CHERD.2007.10.007
869 28. Fissore, D., Pisano, R., & Barresi, A. *Using mathematical modeling and prior knowledge for*
870 *QbD in freeze-drying processes.* In: Jameel F, Hershenson F, Khan MA, Martin-Moe S, eds.
871 Quality by Design for Biopharmaceutical Drug Product Development. New York: Springer.
872 2015; 565-593. https://doi.org/10.1007/978-1-4939-2316-8_23
873 29. Fissore, D., & Pisano, R. *Computer-aided framework for the design of freeze-drying cycles:*
874 *optimization of the operating conditions of the primary drying stage.* Processes, 2015; 3:406-
875 421. http://dx.doi.org/10.3390/pr3020406
876 30. Geidobler, R. & Winter, G. *Controlled ice nucleation in the field of freeze-drying:*
877 *fundamentals and technology review.* Eur. J. Pharm. Biopharm. 2013; 85(2): 214-222.
878 https://doi.org/10.1016/j.ejpb.2013.04.014

Table 1: Values of the heat transfer coefficient K_v obtained through the gravimetric test in MicroFD® and in REVO® freeze-dryer processing water in 2R and in 6R vials. The mean values of the heat transfer coefficient and the standard deviation (given as percentage of the mean value), for each case, are reported.

Pressure, Pa	6.7	13.3	26.7	6.7	13.3	26.7
Vial	6R	6R	6R	2R	2R	2R
$\boldsymbol{K_{v,MicroFD}}$, W m^{-2}K^{-1}	13.5	17.5	25.8	21.4	28.5	37.8
$\boldsymbol{K_{v,MicroFD,bottom}}$, W m^{-2}K^{-1}	17.1	24.4	33.2	23.4	33.4	44.9
$\boldsymbol{K_{v,REVO}}$, W m^{-2}K^{-1}	14.4	18.6	25.8	20.3	30.6	38.3
Standard deviation, % (MicroFD – MicroFD,bottom)	26.7	39.4	28.7	9.3	5.9	18.8
Standard deviation, % (MicroFD,bottom – REVO)	15.8	23.8	22.3	13.2	8.4	14.7
Standard deviation, % (MicroFD – REVO)	6.6	6.2	0.04	5.7	7.0	1.4

Table 2: Heat fluxes calculated for each gravimetric test carried out in the MicroFD® freeze-dryer. Results were obtained processing water in 2R and in 6R vials, at different values of chamber pressure.

Pressure, Pa	6.7	13.3	26.7	6.7	13.3	26.7
Vial	6R	6R	6R	2R	2R	2R
$\dot{Q}_{subl,int}$, W	1.22	1.46	1.59	1.98	2.12	2.66
$\dot{Q}_{base,int}$, W	0.96	1.04	1.24	1.96	1.99	2.42
$\dot{Q}_{LAT}$, W	0.26	0.42	0.35	0.02	0.13	0.24
$\dot{Q}_{subl,ext}$, W	2.94	3.29	3.64	2.67	2.82	3.43
$\dot{Q}_{base,ext}$, W	1.57	2.04	2.07	1.71	1.71	2.24
$\dot{Q}_{LyoSim}$, W	1.62	1.68	1.92	0.98	1.24	1.42

Table 3: Summary of mass transfer parameters. Results were obtained processing a 5% w/w aqueous sucrose solution, in 2R and in 6R vials, in the MicroFD® and REVO® freeze-dryers.

Equipment	MicroFD®	MicroFD®	REVO®
Vial	2R	6R	6R
$\boldsymbol{R_{p,0}}$, m s^{-1}	0	0	0
$\boldsymbol{A}$, s^{-1}	$\mathbf{1.65 \cdot 10^{9}}$	$\mathbf{2.52 \cdot 10^{9}}$	$\mathbf{4.62 \cdot 10^{8}}$
$\boldsymbol{B}$, m^{-1}	$\mathbf{2.02 \cdot 10^{4}}$	$\mathbf{3.76 \cdot 10^{4}}$	$\mathbf{3.61 \cdot 10^{3}}$

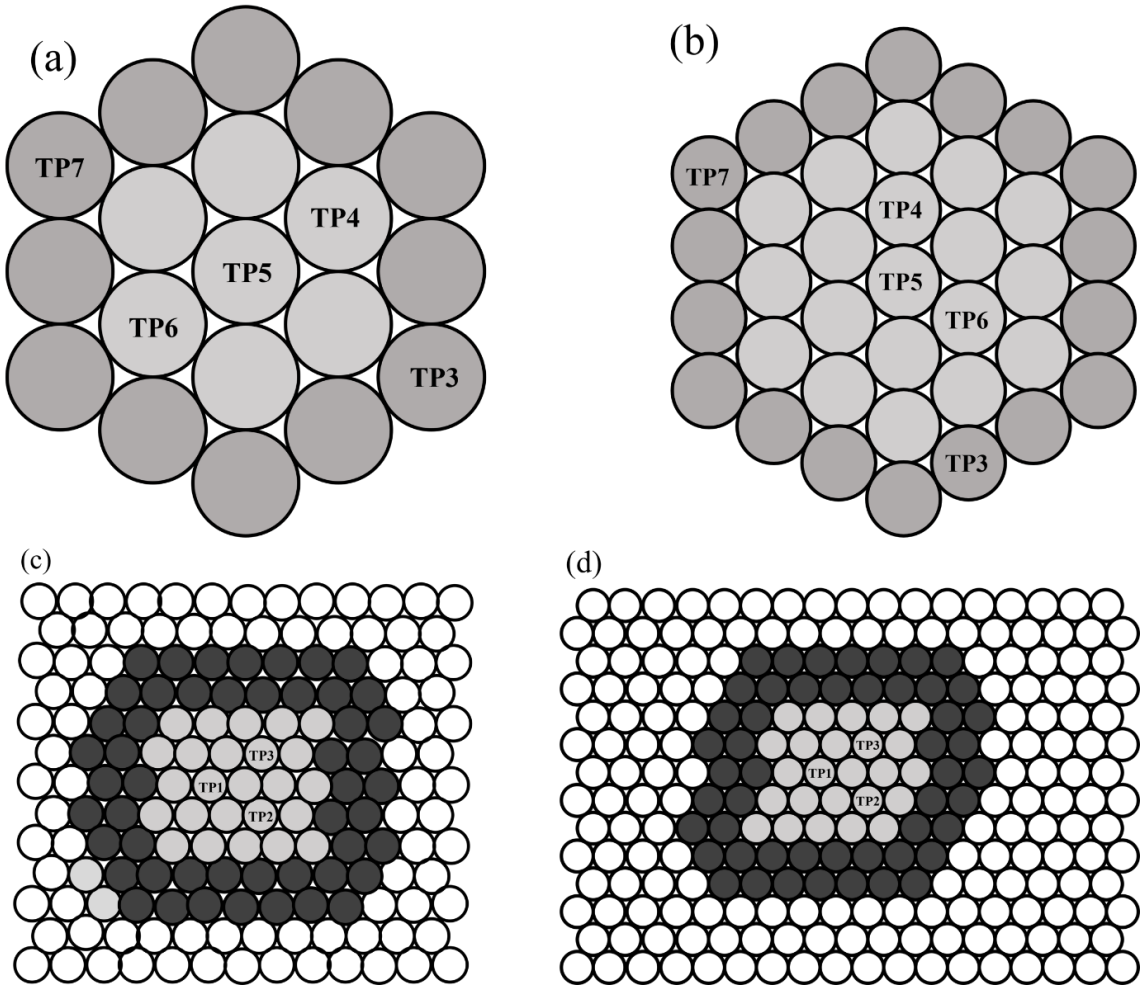

Figure 1: Schematic arrangement of vials and thermocouples for the four configurations used in this study: (a) vials 6R in MicroFD®, (b) vials 2R in MicroFD®, (c) vials 6R in REVO® and (d) vials 2R in REVO®. White circles identify empty vials, black circles identify vials filled with water (or product, depending on the aim of the test), not weighed in the gravimetric test, grey circles identify vials filled with water (or product) and weighed in the gravimetric test. Vials where a thermocouple was inserted are indicated by a label.

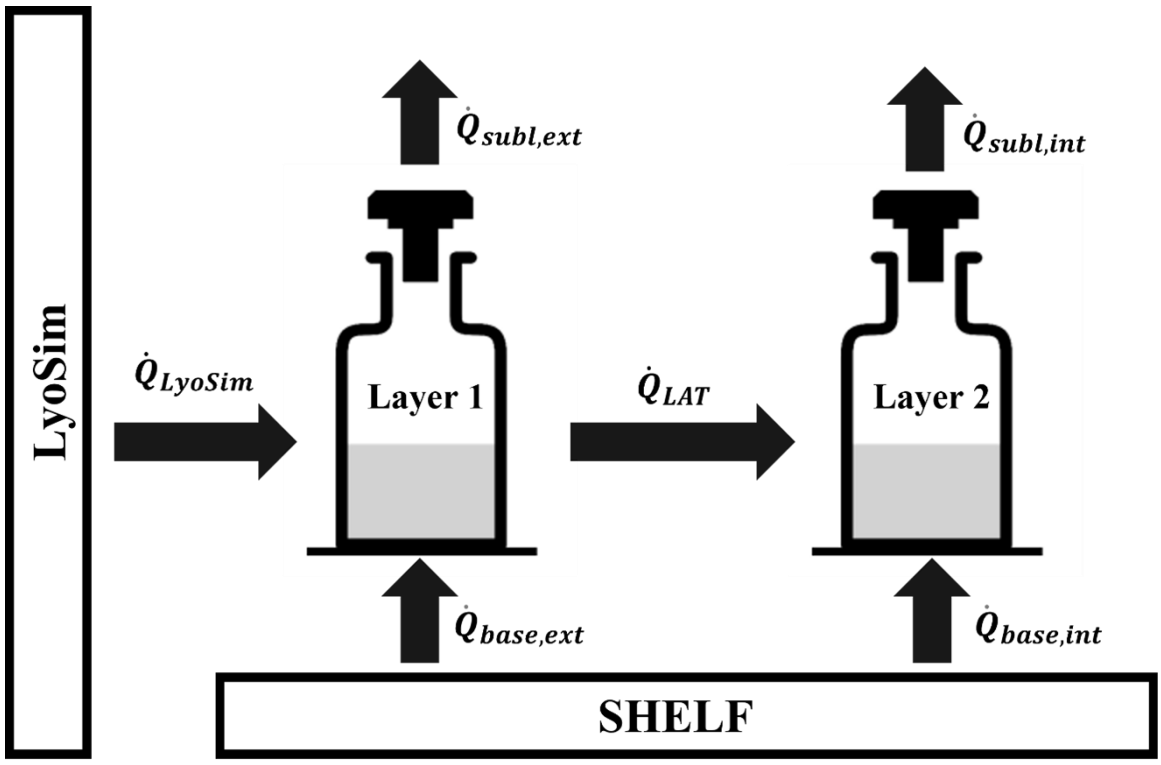

Figure 2: Schematization of the heat fluxes in the MicroFD® freeze-dryer by simplifying the system considering only two layers. The external layer, directly in contact with the ring, is reported as “Layer 1”, while the internal layer as “Layer 2”.

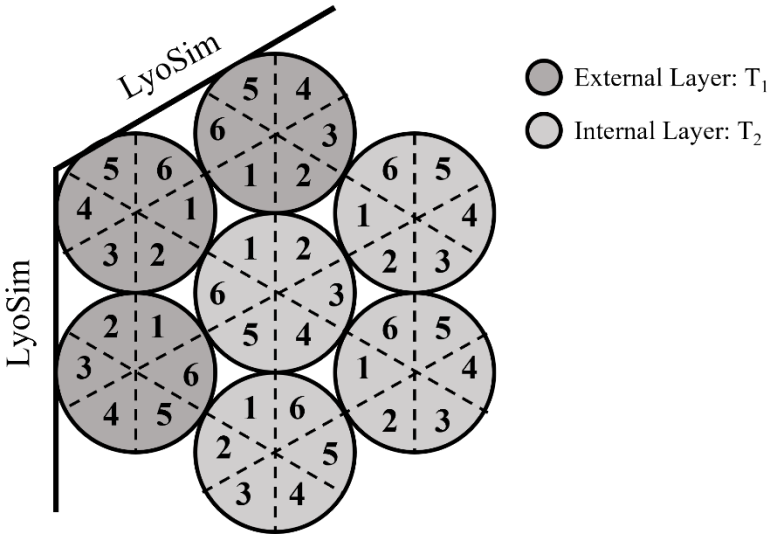

Figure 3: Zoom of the arrangement of 6R vials in MicroFD®.

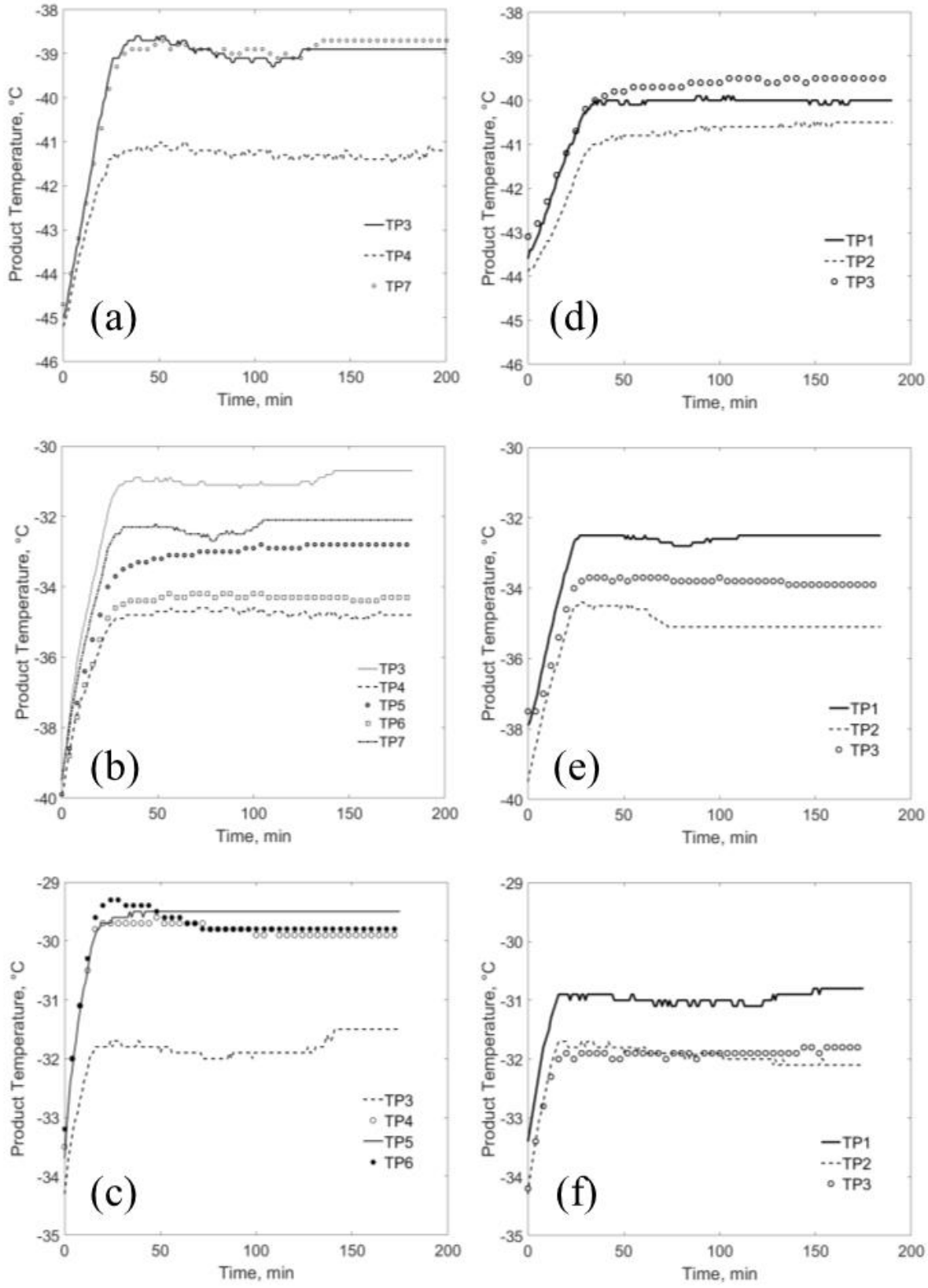

Figure 4: Comparison between the temperature profiles measured in the MicroFD® and in the REVO® freeze-dryers for different values of chamber pressure during the sublimation step. Graphs (a), (b) and (c) refer to tests carried out in the MicroFD® device, while graphs (d), (e) and (f) refer to tests carried out in the REVO® equipment. Results were obtained processing water in 2R vials at the following pressures: (a), (d): 6.7 Pa, (b), (e): 13.3 Pa, and (c), (f): 26.7 Pa. The temperature of the shelf was equal to -10°C and the ring temperature offset was set to 0°C in the MicroFD® freeze-dryer.

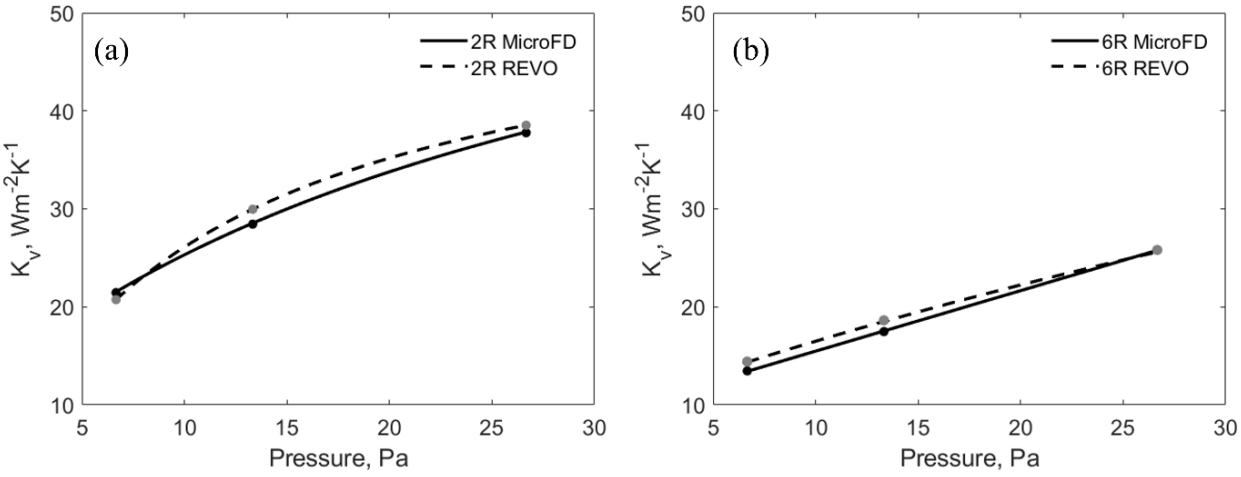

Figure 5: Values of the heat transfer coefficient as a function of chamber pressure for: (a) 2R vials and (b) 6R vials. Results were obtained processing water, in 2R and in 6R vials, in the MicroFD® (solid line) and REVO® (dashed line) freeze-dryers. Symbols identify values obtained through the gravimetric tests, while lines correspond to the curves calculated by minimizing the mean square difference between the experimental and theoretical K_v values (with Eq. 46).

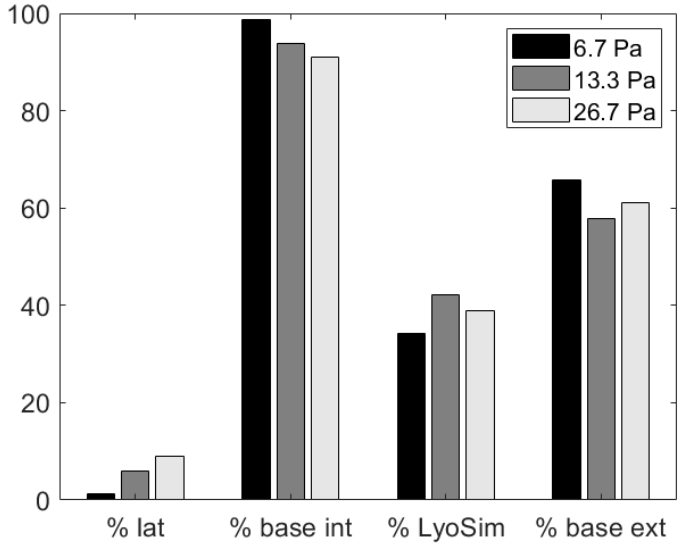

Figure 6: Values of the heat fluxes to the vials in the MicroFD® freeze-dryer, expressed as percentage of the total flux, obtained processing water in 2R vials.

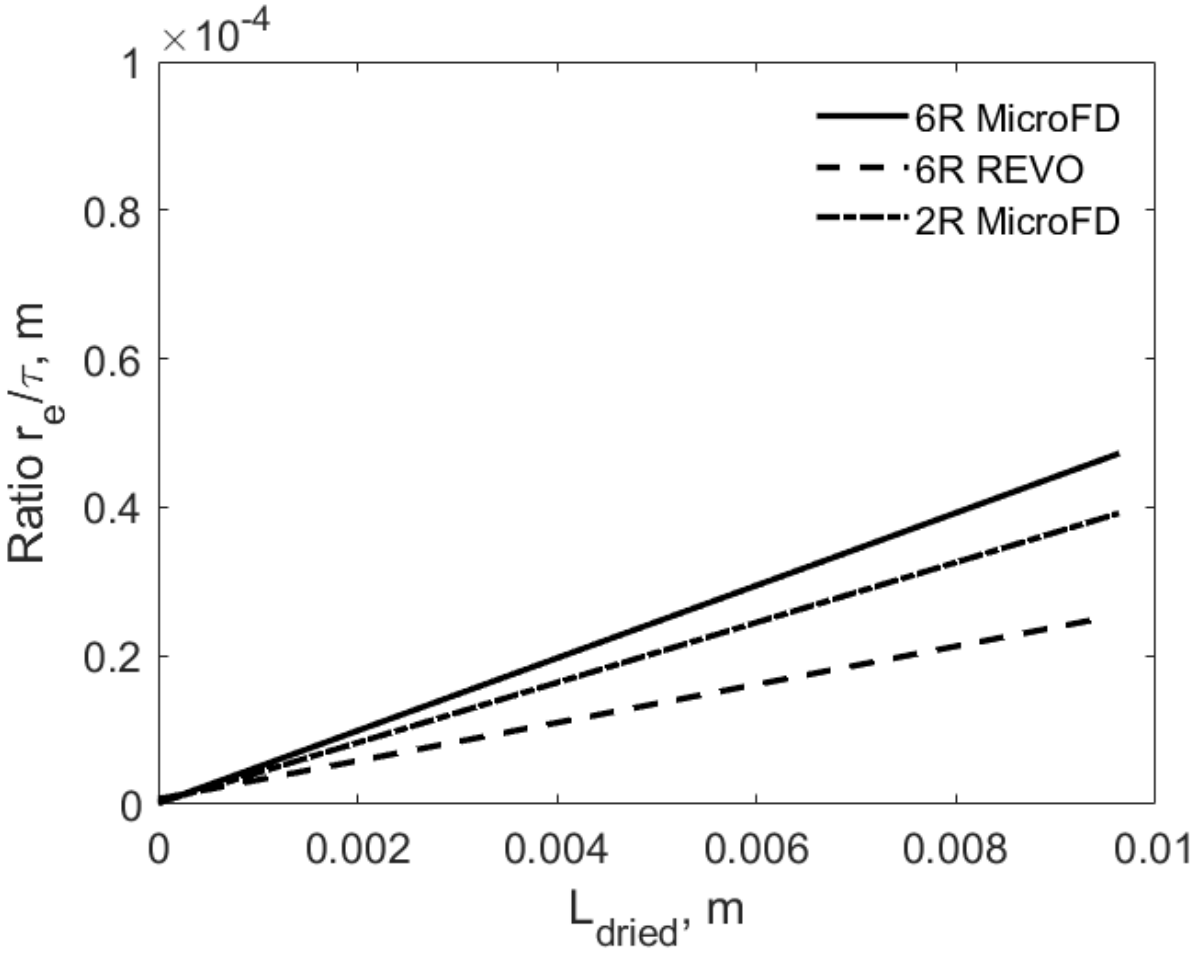

Figure 7: Values of the ratio r_e/τ as a function of the thickness of the dried layer for a 5% w/w aqueous sucrose solution processed in 6R and in 2R vials at 13.3 Pa in a MicroFD® freeze-dryer and in the REVO® freeze-dryer.

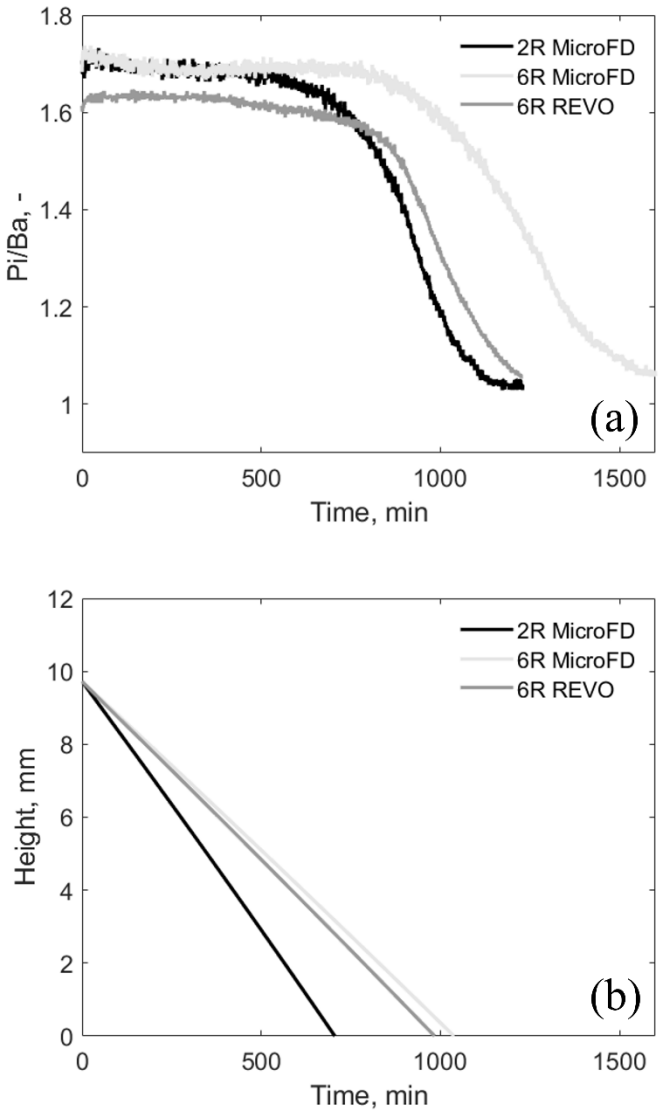

Figure 8: Graph (a): Comparison between the ratio Pirani/Baratron pressure measurements obtained in three tests carried out in the MicroFD® and in the REVO® equipment using 2R (black line) and 6R vials (dark grey and light grey lines). Graph (b): Comparison between the height of the dried cake calculated by the process simulation for the three tests. In all the tests a 5% w/w aqueous sucrose solution was processed at 13.3 Pa. The temperature of the shelf was equal to -10°C and the ring temperature offset was set to -3°C in the MicroFD® freeze-dryer.

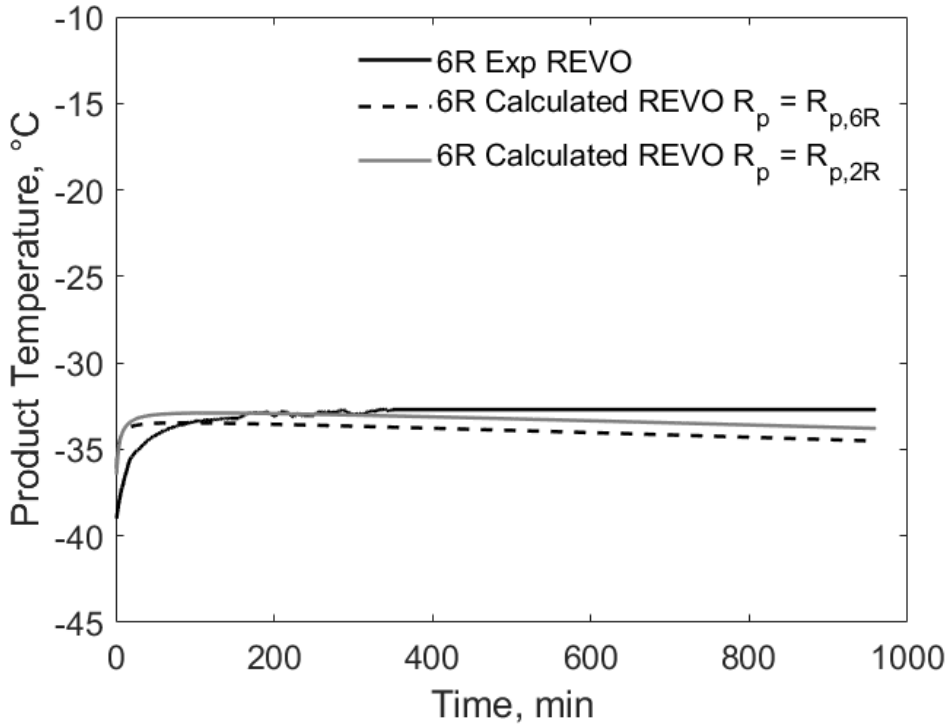

Figure 9: Product temperature in the primary drying stage of a freeze-drying cycle of a 5% w/w aqueous sucrose solution in 6R vials in the REVO® equipment (black line) at 13.3 Pa. The temperature of the shelf was equal to -10°C and the ring temperature offset was set to -3°C in the MicroFD® freeze-dryer. The values obtained through mathematical simulation of the process using the mass transfer parameters calculated for 2R vials in MicroFD® (grey line) and for 6R vials in MicroFD® (dashed line) are also shown. The K_v values found with the optimization algorithm in the first part of the study were used for the mathematical simulations.

Table S1: Weight loss (mean value and standard deviation) in each gravimetric test carried in MicroFD® freeze-dryer.

Pressure, Pa	Vial type	Mean weight loss in vials of layer 1, g	Mean weight loss in vials of layer 2, g	Standard deviation of the weight loss in vials of layer 1, %	D Standard deviation of the weight loss in vials of layer 2, %
6.7	2R	0.6942	0.5077	7.94	7.79
13.3	2R	0.6366	0.4541	8.42	10.12
26.7	2R	0.7480	0.5491	9.19	5.93
6.7	6R	1.0652	0.7603	8.71	2.82
13.3	6R	1.2027	0.888	7.2	4.3
26.7	6R	1.2785	0.9556	7.17	1.48

Table S2: Weight loss (mean value and standard deviation) in each gravimetric test carried in REVO freeze-dryer.

Pressure, Pa	Vial type	Mean weight loss, g	Standard deviation of the weight loss in vials, %
6.7	2R	0.3837	6.06
13.3	2R	0.4510	7.54
26.7	2R	0.4682	7.81
6.7	6R	0.6158	12.19
13.3	6R	0.6802	6.77
26.7	6R	0.5624	5.06

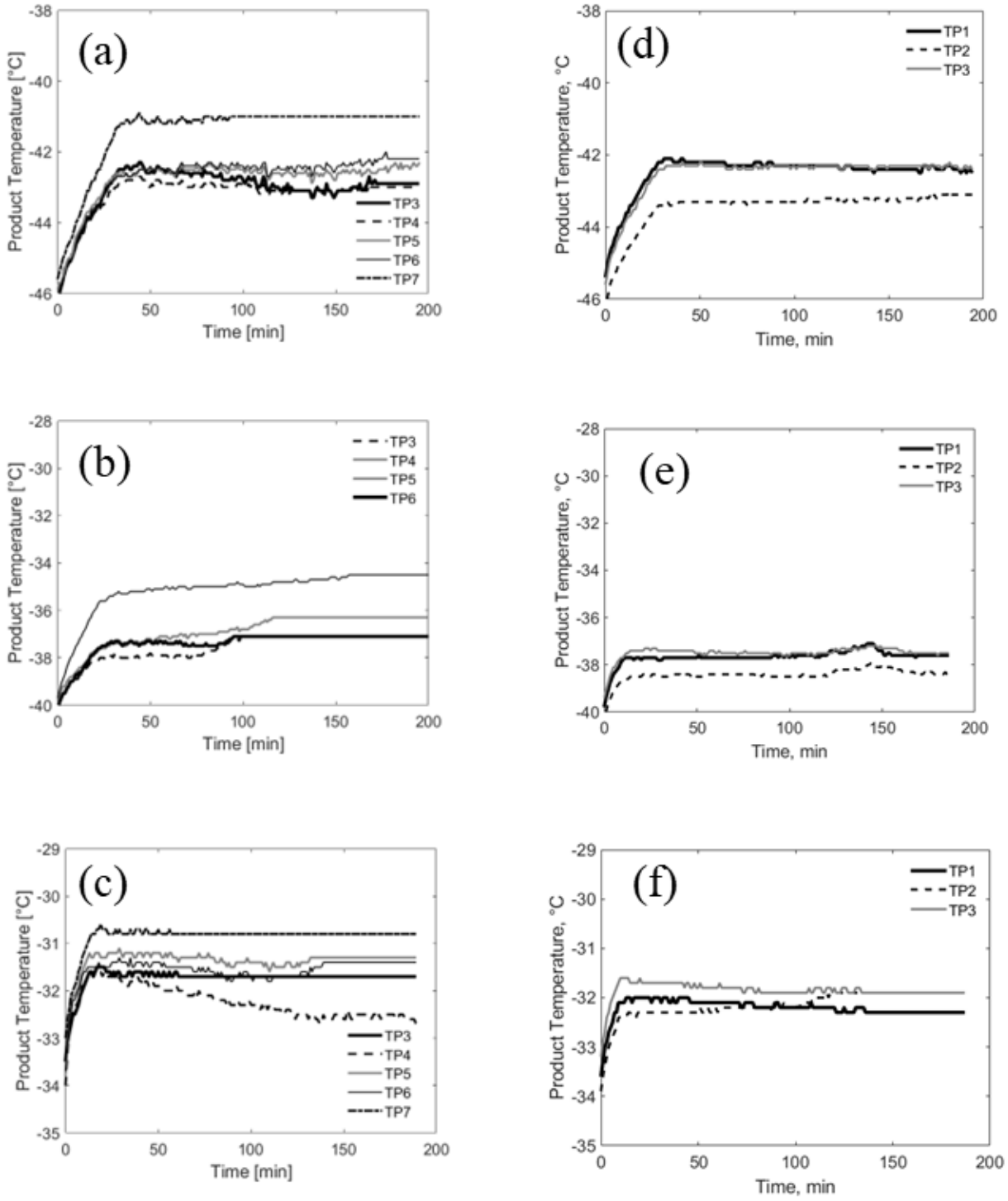

Figure S1: Comparison between the temperature profiles measured in the MicroFD® and in the REVO® freeze-dryers for different values of chamber pressure during the sublimation step. Graphs (a), (b) and (c) refer to tests carried out in the MicroFD® device, while graphs (d), (e) and (f) refer to tests carried out in the REVO® equipment. Results were obtained processing water in 6R vials at the following pressures: (a), (d): 6.7 Pa, (b), (e): 13.3 Pa, and (c), (f): 26.7 Pa. The temperature of the shelf was equal to -10°C and the ring temperature offset was set to 0°C in the MicroFD® freeze-dryer.

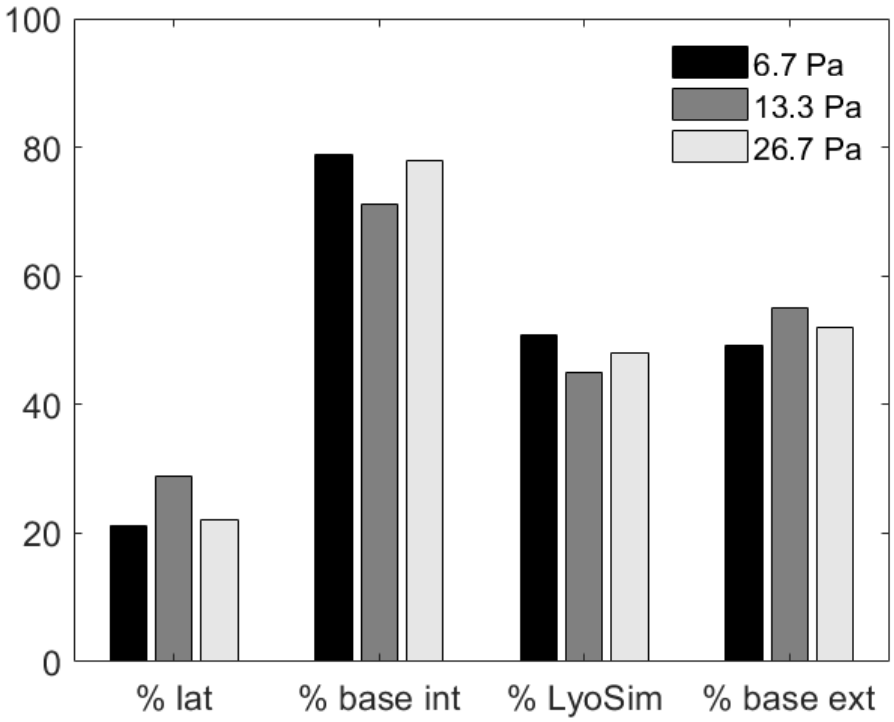

Figure S2: Values of the heat fluxes to the vials in the MicroFD® freeze-dryer, expressed as percentage of the total flux, obtained processing water in 6R vials.

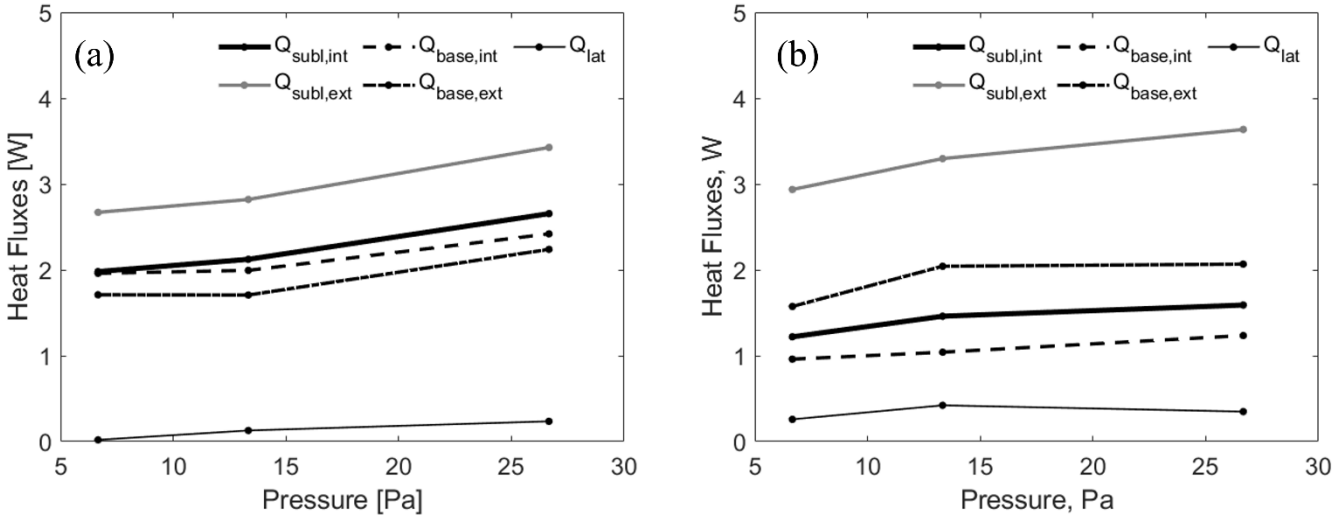

Figure S3: Comparison between the values of the heat fluxes to the vials in the MicroFD® freeze-dryer as a function of chamber pressure for (a) 2R vials and (b) 6R vials. Results were obtained by processing water in the MicroFD® freeze-dryer for three values of chamber pressure: 6.7, 13.3 and 26.7 Pa. The temperature of the shelf was equal to -10°C and the ring temperature offset was set to 0°C.

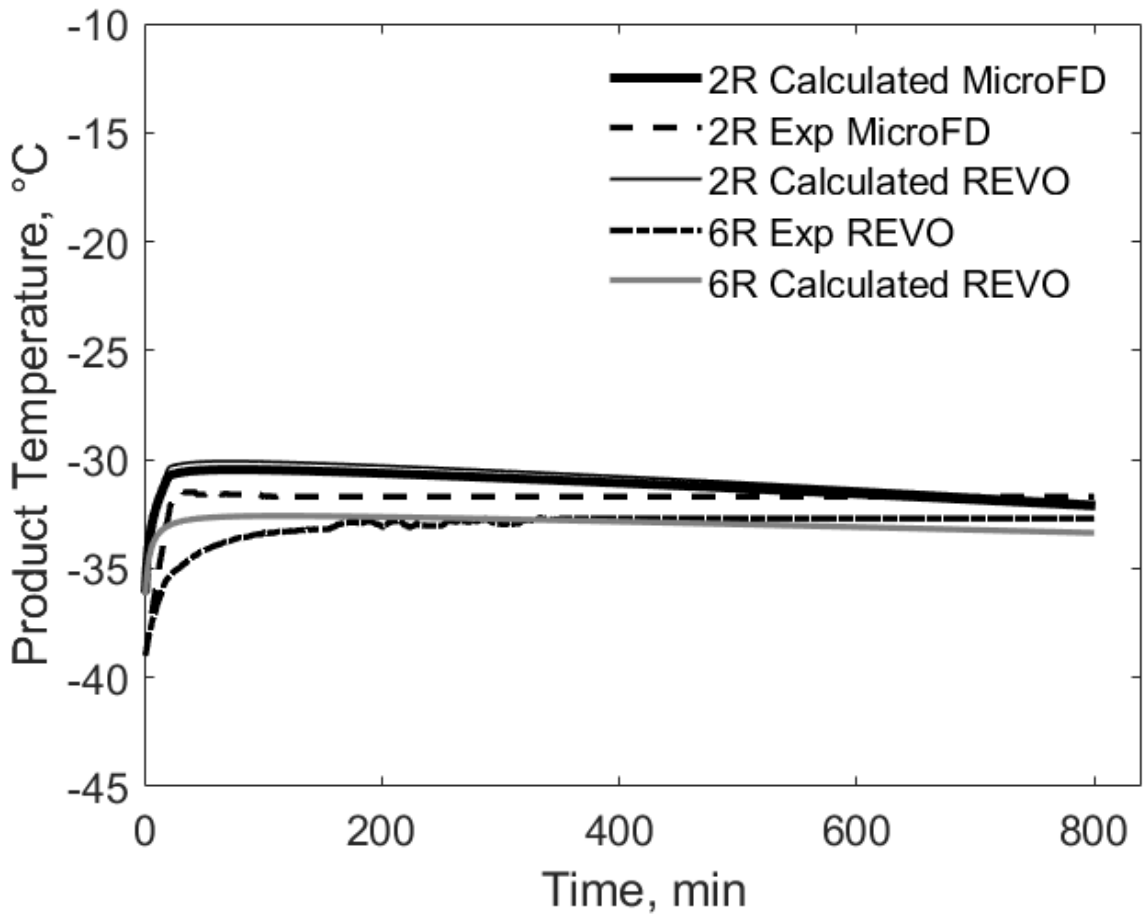

Figure S4: Product temperature profiles measured by means of a thermocouple in a vial during the primary drying stage of a 5% w/w aqueous sucrose solution in 6R vials in the REVO® equipment (stretch point black line) and in 2R vials in the MicroFD® (dashed black line) at 13.3 Pa. The temperature of the shelf was equal to -10°C and the ring temperature offset was set to -3°C in the MicroFD® freeze-dryer. Values are compared with those obtained by process simulation using the experimental mass transfer parameters calculated for 2R vials in MicroFD® (grey line) and by simulating the behavior of the 2R vials using all the experimental parameters obtained in the MicroFD® (thick black line). The calculated trend in the 2R vials using the K_v value found in the first part of the study in the REVO® equipment is also shown for comparison (black line).